Application of a new small RNA molecule, RNA-LZ-1, as a vaccine adjuvant

A Thesis Submitted to the College of

Graduate and Postdoctoral Studies

In Partial Fulfillment of the Requirements

For the Degree of Master of Science

In the Vaccinology and Immunotherapeutics Program

School of Public Health

University of Saskatchewan

Saskatoon, SK

By

Magda Hlasny

Permission to use

In presenting this thesis in partial fulfillment of the requirements for a postgraduate degree from the University of Saskatchewan, I agree that the libraries of this university may make it freely available for inspection. I further agree that permission for copying of this thesis in any manner, whole or in part, for scholarly purposes may be granted by the professors who supervised my thesis work or in their absence, the Head of the Department or the Dean of the college in which my thesis work was done. It is understood that any copying or publication or use of this thesis or parts thereof for financial gain shall not be allowed without any written permission. It is also understood that due recognition shall be given to me and to the University of Saskatchewan in any scholarly use which may be made of any material in my thesis.

Request for permission to copy or to make other use of material in this thesis in whole or part should be addressed to:

Executive Director, School of Public Health,

Program Director, Vaccinology and Immunotherapeutics

University of Saskatchewan

107 Wiggins Road

Saskatoon, Saskatchewan, S7N 5E5

Canada

Abstract

Influenza A viruses are important pathogens that cause disease in a wide variety of species leading to economic losses and added burden on health care. Recently, outbreaks of avian influenza viruses in the human population have added to this growing risk of pandemic influenza viruses. Therefore, strategies to address the demands of higher efficiency, immunogenicity, and safety in influenza vaccines must be explored. One strategy which addresses efficiency and immunogenicity is to explore the addition of an adjuvant to influenza vaccines.

Adjuvants are commonly used vaccine components which are included to induce a robust immune response leading to antigen sparing, a broader spectrum of protection and the elimination of a booster. Recently the retinoic acid-inducible gene-I (RIG-I) pathway, which is the natural defense against RNA viruses, has become an attractive target for adjuvant development. In this thesis, we sought to explore the possibility of a small RNA molecule, RNA-LZ-1, identified in our laboratory as a RIG-I agonist as an adjuvant.

This project evaluated the induction of pro-inflammatory cytokines, chemokines, and interferons by RNA-LZ-1 *in vitro* and *in vivo*, and tested its ability to induce antigen-specific antibodies when paired with H5N1 and H7N9 inactivated whole influenza viruses. We hypothesized that due to RNA-LZ-1's binding affinity for RIG-I it will induce a broad spectrum immune response and fortified adaptive response when used as an adjuvant. Overall our results showed that RNA-LZ-1 was capable of inducing activation of a diverse spectrum of inflammatory genes and proteins *in vitro* and *in vivo.* In human macrophages and lung epithelial cells RNA-LZ-1 induced significant levels of IFN-β protein and mRNA fold change. We also showed that as early as 3 hours post-injection, RNA-LZ-1 was capable of up-regulating immune

genes with the effect dissipating by 48 hours post-injection. These immune genes were grouped as follows cytokines (IL-12α, IL-12β, IL-6, and IL-18), chemokines (MIP-1α, RANTES, MIP-2, MCP-1, and IP-10), and interferons (IFN-α, IFN-β, and IFN-γ). The overall immune response observed was skewed towards a Th1 response. *In vivo,* RNA-LZ-1 was able to induce protective antigen-specific antibodies against H5N1 in comparable levels to the proven VIDO triple adjuvant showing that RNA-LZ-1 is a strong candidate as an adjuvant for influenza vaccines.

Acknowledgements

I would first like to thank my supervisor Dr. Yan Zhou for giving me the opportunity to broaden my knowledge and skills in the research field. This master's provided me with the opportunity to learn new things, meet new people, and expand my understanding of science. I will always value the knowledge I have gained in the Zhou lab. Secondly, I would like to thank my committee member Dr. Heather Wilson and my chair Dr. Suresh Tikoo for always providing valuable information and pushing me to do better through observations and thoughtful questions and suggestions.

I would also like to acknowledge my colleagues past and current, who made my time here enjoyable and always lent a helping hand, whether with an experiment or answering questions I had. They made the years go by in the blink of an eye. Specifically, I would like to thank Leonard Liu and Hyun-Mi Pyo, who spent countless hours teaching me and helping me increase my knowledge surrounding my project. Their contributions will always be greatly appreciated. And to Jocelyne, Yao, and Janet for all the supper and board game nights we have enjoyed throughout the years, hopefully they will continue into the future. I would like to thank the help I received from Laura Latimer, Marlene Snider, and all of the animal care staff, whom aided in the smooth running of my animal trials.

Finally, I would like to thank my parents Ron and Heather Hlasny and my husband Michael Langton for always encouraging me to follow my dreams and supporting me every step of the way throughout this degree. Without them I would not be the person I am today and for that I thank them greatly.

Cheers,

Magda

Table of Contents

List of figures

List of equations and tables

List of abbreviations

APC	Antigen Presenting Cells
BSA	Bovine Serum Albumin
CARD	Caspase Recruitment Domain
CTD	C Terminal Domain
DEPC	Diethylpyrocarbonate
dsRNA	Double Stranded RNA
FDA	Food and Drug Administration
GFP	Green Fluorescent Protein
HA	Hemagglutinin
HAI	Hemagglutinin Inhibition
IFN	Interferon
IL	Interleukin
IRF3	Interferon Regulatory Factor 3
ISCOM	Immune Stimulating Complexes
LGP2	Laboratory of Genetics and Physiology 2
M	Matrix Protein
M2	Matrix Protein 2 Ion Channels
MAVS	Mitochondrial Antiviral-Signaling Protein
MDA5	Melanoma Differentiation-Associated Gene 5
MOI	Multiplicity of Infection
NA	Neuraminidase
NACI	National Advisory Committee on Immunization
NF-κB	Nuclear Factor-κB
NP	Nucleoprotein
NS	Non-Structural Protein
PMA	Phorol Myristate Acetate
PRR	Pattern Recognition Receptor
RBC	Red Blood Cells
RDE	Receptor Destroying Enzyme
RIG-I	Retinoic-acid Inducible Gene-I
RLR	RIG-I-Like Receptor
TLR	Toll Like Receptor
VIDO-InterVac	Vaccine and Infectious Disease Organization – International Vaccine Center
VLP	Virus Like Particle
QS21	Detoxified Saponin Derivative

Chapter 1 Introduction

1.1 Influenza virus

1.1.1 Genome and proteins

Influenza A virus is part of the *orthomyxoviridae* family which is comprised of single-stranded negative sense RNA viruses that do not develop long-term host-virus relationships, as the virus does not become dormant at any point in the life cycle (Jenigan & Cox, 2013). Influenza A viruses have a broad host range including humans, wild and domestic birds, swine, equine, canine, feline, and seals to name a few (Klenk, Garten, & Matrosovich, 2013). The genome consists of eight segments, encoding for both structural and non-structural proteins, which are numbered one through eight by decreasing length (Bouvier & Palese, 2008). These segments are located in the virus core and are enveloped by matrix protein (M1) coated with a lipid bilayer and ion channels (M2) (Krug & Fodor, 2013). Attached to the lipid bilayer of the virus are hemagglutinin (HA) and neuraminidase (NA) surface glycoproteins at a ratio of four to one, respectively (Bouvier & Palese, 2008). HA being the most abundant surface glycoprotein is involved in the binding of the virus to the host's sialic acid-containing receptors. NA, the other surface glycoprotein also interacts with sialic acid receptors by removing the sialic acid from the virus during virus budding from host cells (Krug & Fodor, 2013). These glycoproteins are where influenza virus strains derive their nomenclature from, an example is the H1N1 and H3N2 strains, where the H stands for the subtype of hemagglutinin protein and the N is the subtype of neuraminidase protein (Bouvier & Palese, 2008).

The largest RNA segments in the influenza A genome encode for the three polymerase proteins, segment 1 PB2, segment 2 PB1, and segment 3 PA (Krug & Fodor, 2013). However, segments 2 and 3 also encode for other proteins besides those involved in the polymerase

complex. Segment 2 encodes for two other proteins besides PB1, these are PB1-F2, which is a pro-apoptotic virulence factor, and PB1-N40, which is a truncated version of PB1 that is recently discovered. PA also encodes for a second protein through ribosomal frameshifting called PA-X, which has been shown to modulate virulence (Krug & Fodor, 2013). The next three segments in the influenza A genome only encode for a single protein, these are segment 4 HA, segment 5 nucleocapsid protein (NP), and segment 6 NA (Krug & Fodor, 2013). Above we briefly described that HA and NA are surface glycoproteins involved in both the binding and budding of the virus, respectively. NP encapsulates the viral RNA located in the virus core and also plays a role in viral RNA replication. The last two segments 7, matrix protein (M), and 8, non-structural protein (NS), are spliced and the resultant mRNAs, spliced and un-spliced, are both translated (Krug & Fodor, 2013). The M segment encodes for M1 which as described above lies underneath the lipid membrane as part of the envelope, and M2 which encodes for the ion channels present in the lipid membrane and aid in the un-coating of the virus. For segment 8, the un-spliced mRNA encode for non-structural protein NS1 and the spliced mRNA encodes for two proteins involved in nuclear export, NS2 and NEP (Krug & Fodor, 2013).

1.1.2 Hemagglutinin protein

Influenza A HA is highly antigenic and these antigenic differences have led to the categorization of 18 HA subtypes named H1 – H18 ("Influenza Type A Viruses,"). HA subtypes H1 - 16 are capable of infecting avian species, whereas bats are the known host for H17 and H18 virus strains ("Influenza Type A Viruses,"). HA is a membrane fusion protein located on the lipid membrane of the envelope that carries antigenic sites on the head domain. HA is initially found as the precursor HA0 which is cleaved into HA1 and HA2 (Skehel & Wiley, 2000). HA1 is the head domain and is involved in binding to target cell receptors and is the location of the

antigenic sites and antibody binding (Lai & Freed, 2015; Skehel & Wiley, 2000). HA2 contains the fusion peptide, which catalyses membrane fusion and also has the transmembrane domain that anchors HA to the viral membrane (Lai & Freed, 2015).

In the virus life cycle, HA has two roles the first being receptor binding to sialic acid receptors and the second being a membrane fusion protein (Gamblin & Skehel, 2010). Inside the host cell the virus replicates HA mRNA which is transcribed into HA0. HA0 is cleaved and becomes the two polypeptide chains HA1 and HA2. On the N-terminal of HA2 the fusion peptide is located and after refolding it forms the trimer interface, by which HA can now form a trimer (Gamblin & Skehel, 2010). Before the virus enters a host cell, HA recognizes the sialic acid receptors and binds to them initiating entrance to the host cell. There are two different sialic acid receptors: α(2,6) linkage which is recognized by influenza viruses of human origin and α(2,3) linkage which is recognized by viruses of avian origin (Skehel & Wiley, 2000). After receptor binding, HA mediates the fusion between the virus and the endosomal membrane in order to deliver the viral genome into the cell for replication. Release of the viral genome occurs by repositioning of the fusion peptide leading to a structural change in HA that creates a bridge between the virus and endosomal membrane (Gamblin & Skehel, 2010).

1.1.3 Symptoms, pathogenesis, and transmission

Influenza A virus can infect all age groups of people causing a wide range of respiratory infection from subclinical infections to the onset of lethal pneumonia (Nichelson, 1998). Persons at higher risk for hospitalization and possible complications due to infection include young children, the elderly, pregnant women, and those whom are immunocompromised (Hayden & de Jong, 2013). However, in uncomplicated influenza A infection, generally with the seasonal strain, symptoms usually include systemic symptoms such as fever, chills, and muscle pain, and

respiratory symptoms such as dry cough, a runny or plugged nose, and a sore throat. Persons usually present with a fever the day after infection followed by other systemic symptoms, which begin to dissipate three to four days presentation being replaced by the respiratory symptoms (Nichelson, 1998). After the systemic symptoms disappear persons will still feel lethargic and may take up to a couple weeks to resume higher intensity activities, such as exercising and sports (Hayden & de Jong, 2013).

Influenza A infection can lead to complications or secondary infections in some people. The main complication with influenza infection is pneumonia, there are two types of pneumonia (McCullers, 2011). Primary influenza viral pneumonia is more commonly found in children and leads to respiratory failure, which can lead to mortality with rates of 25-50%. However, the implementation of an early antiviral treatment can decrease the mortality rate (Hayden & de Jong, 2013). Viral pneumonia was present in 50% of admitted patients infected with the 2009 pandemic H1N1 virus or with the recently emerging avian H5N1 and H7N9 viruses. Epidemiologic analysis show that persons who develop viral pneumonia commonly have pre-existing cardiac or pulmonary conditions, however, this is not the case for the 2009 pandemic virus and avian viruses (Hayden & de Jong, 2013). A second type of pneumonia experienced by influenza A-infected individuals is bacterial pneumonia. This occurs after people have acquired a secondary bacterial infection, most commonly caused by *Streptococcus pneumoniae (Palacios et al., 2009)*. Bacterial pneumonia is the most common complication in influenza A infected persons. During the 1918 pandemic with Spanish influenza all most every fatal reported case was due to bacterial pneumonia, and in the following 1957 and 1968 pandemics 70% of life-threatening pneumonia cases were caused by bacterial pneumonia. However, both viral and

bacterial pneumonia are more likely to occur in infected persons with underlying conditions (Hayden & de Jong, 2013).

Transmission of influenza A in humans occurs through the release of respiratory secretions containing virus by coughing or sneezing. Infection in the upper and lower respiratory tract can occur from influenza A virus present in both large droplets and small aerosols from an infectious person traveling far distances to the new recipient (Ladhani et al., 2017). Human infection by avian, swine, and other species can occur through direct contact with the infected animal, including their waste. The initial site of infection for influenza A is the respiratory mucosa (Hayden & de Jong, 2013). Human influenza A viruses have preferential binding to the α2,6-linked sialic acid receptors, whereas avian strains preferentially bind α2,3-linked sialic acid receptors (Mair, Ludwig, Herrmann, & Sieben, 2014). In the human lung both the upper and lower respiratory tract are abundant in α2,6-linked sialic acid receptors compared to the α2,3-linked sialic acid receptors, which are only found in the distal bronchioles. The distribution pattern of sialic acid receptors is one factor that could affect the pathogenicity of human versus avian influenza A strains (Mair et al., 2014). Avian viruses would therefore have more difficulty finding receptors to bind in a human host due to the depth of the lung the virus must reach to interact with the α2,3-linked sialic acid receptors.

1.2 Influenza vaccines

1.2.1 Vaccines currently available

Every year for seasonal influenza the World Health Organization releases their recommendations on strains to be included in the vaccine for the upcoming fall in February of the same calendar year. Once the recommendation has been released the Influenza Working Group develops the vaccines to be distributed in Canada and submits them to the National

Advisory Committee on Immunization (NACI) for consideration. In Canada, only two categories of vaccines are authorized for use, they are inactivated and live attenuated vaccines ("Canadian immunization guide chapter on influenza and statement on seasonal influenza vaccine for 2016-2017," 2017).

Inactivated vaccines used against influenza viruses in Canada are a mixture of split virus and subunit vaccines. Split virus vaccines contain virus that has been disrupted by a detergent. Subunit vaccines consist of the HA and NA proteins with the viral components removed ("Canadian immunization guide chapter on influenza and statement on seasonal influenza vaccine for 2016-2017," 2017). Trivalent and quadravalent inactivated vaccines are authorized in Canada. In the trivalent vaccines there are two influenza A strains and one influenza B strain and in the quadravalent a second influenza B strain is added to the formulation ("Canadian immunization guide chapter on influenza and statement on seasonal influenza vaccine for 2016-2017," 2017). In adults over the age of 65, an inactivated vaccine containing 60 μg of HA protein in comparison to the 15 μg of HA protein administered to persons under 65 years of age. This elevated antigenic dose is administered to seniors because they sometimes need higher levels of antigen to invoke the desired immune response (Kumar et al., 2017). Children under two years of age are also considered a low responder group and they are administered an inactivated vaccine, which has the adjuvant MF59 is added. MF59 is a squalene oil in water emulsion, which is stabilized through the addition of surfactants (Mosca et al., 2008). MF59 is capable of decreasing the amount of influenza antigen needed for vaccination and provide enhanced and extended antibody titres (O'Hagan, 2007).

The live-attenuated influenza vaccine is recommended for persons between the ages of 2 and 59. It is an intranasal spray in which the influenza strains are attenuated and cold-adapted so

that they will only replicate in the nasal mucosa versus the lungs ("Canadian immunization guide chapter on influenza and statement on seasonal influenza vaccine for 2016-2017," 2017). FluMist® is quadravalent and has proven to have the highest efficacy compared to inactivated influenza vaccines in the designated age range mentioned above ("Canadian immunization guide chapter on influenza and statement on seasonal influenza vaccine for 2016-2017," 2017). Overall vaccination against influenza is highly recommended especially in the high-risk groups such as, persons with chronic health conditions, pregnant women, the elderly, infants, and aboriginal peoples.

1.2.2 Experimental vaccines

Since current vaccines are mainly developed with whole inactivated or live attenuated viruses, the antibody response is mainly biased towards the HA head region (Kim et al., 2017). The HA region is highly variable and therefore antibodies produced against one strain are not cross-reactive against the evolving virus. The overarching goal in influenza vaccine development is to create a universal vaccine that would provide broad spectrum protection across strains (Impagliazzo et al., 2015). These vaccines can include virus-like particle vaccines, chimeric HA vaccines, and HA stem targeting vaccines.

Virus-like particle (VLP) vaccines are a more favourable alternative to the currently used live attenuated and split vaccines. The general description of VLP is that they mimic the virus structure and morphology without being infectious (Beljanski et al., 2015). The components of the vaccine include a strong glycoprotein immunogen, such as HA, and a potent adjuvant (Osterholm, Kelley, Sommer, & Belongia, 2012), and include NA and M proteins (Beljanski et al., 2015). Because they are non-infectious, they have excellent safety profile in comparison with currently available vaccines. Another advantage of VLP vaccines is that they

can be engineered to contain multiple antigens, allowing them to represent a broader population of strains (Beljanski et al., 2015). Overall these attributes make VLPs an attractive vaccine alternative to live-attenuated or split vaccines currently used.

Chimeric vaccines are another experimental vaccine. Generally, the HA is the protein being mutated, an example is a chimeric H9 H5 vaccine where the head domain is derived from H9 and the stalk domain is derived from H5 (Kim et al., 2017). These vaccines account for the production of antibodies against both the head domain and stalk domain of HA. Although the stalk domain is less immunogenic due to its position on the virus, it is highly conserved throughout the different subtypes of HA (Kim et al., 2017). Experimental research showed that a chimeric vaccine was able to protect from lethal challenge against both avian H9N2 and H5N1 viruses (Kim et al., 2017) because the host responded with production of antibodies against both the head and stalk domains of HA. Therefore, the main advantage of chimeric vaccines is that cross-protection is achieved against both virus subtypes utilized.

Another experimental vaccine is one in which the highly-conserved HA stem is used as the vaccine antigen and it is the type of vaccine most people associate with a universal vaccine (Impagliazzo et al., 2015; Kim et al., 2017). Antibodies produced against the influenza A HA stem region are referred to as broadly neutralizing human monoclonal antibodies and were recently discovered, raising hope for a universal vaccine candidate (Corti et al., 2011; Ekiert et al., 2009; Ekiert et al., 2011). The construction of the HA stem alone has been challenging as the removal of the transmembrane domain and globular head domain lead to the loss of structural confirmation (Cohen, 2013). Therefore, even though large portions of HA are being deleted the stem antigen must maintain stability and structural resemblance to the full-length HA (Impagliazzo et al., 2015). There have been successful attempts at creating HA stem antigens

that induce the broadly neutralizing antibodies (Impagliazzo et al., 2015), however, there is still more experiments to be done to establish these as plausible universal vaccines. The major advantage of using the HA stem domain is the production of broadly neutralizing antibodies, however, the disadvantage is that the stem region is less immunogenic and therefore will need to be paired with a strong adjuvant.

1.3 Adjuvants

1.3.1 Purpose of adjuvants

An adjuvant can be a natural or synthetic compound that is used to increase the immune response to a paired antigen (Alving, Peachman, Rao, & Reed, 2012; Awate, Wilson, Lai, Babiuk, & Mutwiri, 2012). Specifically, an ideal adjuvant will increase the quality, longevity, potency, and specificity of the immune response to the antigen (Alving et al., 2012). Vaccines are formulated to include adjuvants that are specifically tailored to promote the type of immune response most likely to clear the virus, bacteria or fungus (Alving et al., 2012). For example, retinoic-acid inducible gene I (RIG-I) ligands are involved in host defense against RNA viruses and therefore may be ideal adjuvants to include in antiviral vaccines (Patel & Garcia-Sastre, 2014). Overall, an adjuvant should induce a robust immune response, including both humoral and cell mediated responses. The ratio of humoral versus cell mediated response depends on the type of pathogen, against the antigen and lead to antigen sparing and the elimination of a booster (Awate et al., 2012; Sivakumar, Safhi, Kannadasan, & Sukumaran, 2011). For example, if your vaccine is against tuberculosis you would want an adjuvant with an immune response skewed towards cell mediated, whereas for influenza you would want a response skewed towards a humoral response.

There are different types of adjuvants available to choose from depending on the immune response or delivery method desired for the paired antigen. Many of these adjuvants can be combined to increase the effectiveness of the desired response. For example liposomes generally contain cholesterol, for the purpose of binding and detoxifying saponins, a naturally derived product from tree bark, which are also an immune stimulated complex (ISCOM) (Sivakumar et al., 2011). The quenching of the toxic component by the cholesterol causes the toxic component to punch holes in the lipid layer instead of the cell membranes causing the release of the antigen (Alving et al., 2012). Adjuvants are also chosen for the immune response they elicit, which depending on the pathogen could be skewed to either Th1 or Th2 immune response. Mineral salts, which have been used for over a decade as adjuvants due to their potency (Sivakumar et al., 2011), tend to have an immune response skewed towards Th2 (Mosca et al., 2008). As mentioned in the above paragraph the ability to reduce the amount of antigen used is a key feature of a good adjuvant. Oil-in-water emulsions have an antigen dose sparing effect by activating local immune cells leading to increased antigen presentation (Alving et al., 2012; Sivakumar et al., 2011). Some adjuvants due to their toxicity are only justifiable in certain situations for example cytokines, such as granulocyte-macrophage colony stimulating factor have been used to induce antigen presenting cells and primary immune response, making them useful in cancer vaccines, however, they are quite toxic which limits there use in other human vaccines (Sivakumar et al., 2011). Finally micro-particle adjuvants are usually biodegradable polymers which can be used to deliver the antigen to specific regions and be designed to allow for slow or gradual release of the antigen (Sivakumar et al., 2011). Micro-particles are therefore an example of an adjuvant which is used due to its ability to deliver antigens specifically and allow for depot effect.

1.3.2 Adjuvants currently available

Since adjuvants are capable of increasing the immune response to paired antigens there have been many developed and approved for use in humans with specific vaccines. An example of a liposome adjuvant system used in a malaria vaccine is AS01S or AS01B. It is comprised of liposomes from detoxified monophosphorys lipid A and a detoxified saponin derivative (QS21) which are quenched by cholesterol. In this case the component to exert toxicity to make holes in the lipid layer is QS21 (Alving et al., 2012). AS02A is similar to the adjuvants mentioned above except squalene interacts with the cholesterol, which has shown to enhance stability and improve the overall effect of the adjuvant (Alving et al., 2012). Epaxal is a liposome based hepatitis A vaccine that induces both cellular and humoral immunity and lead to long term immunity (Sivakumar et al., 2011). Alum, which is a commonly used adjuvant due to its long history of use, can be derived from either aluminum hydroxide or aluminum phosphate. It has a short-term depot effect, induces a strong Th2 response, and can enhance uptake of the antigen by antigen presenting cells (Mosca et al., 2008; Sivakumar et al., 2011). The two main oil-in-water adjuvants available are MF59 and AS03, they contain 2% squalene and AS03 also contains vitamin E (Alving et al., 2012). MF59 and AS03 increase the uptake of antigen by antigen presenting cells and also have an antigen sparing effect (Alving et al., 2012). Even though many adjuvants are available for use in human vaccines, there is still much to be learned about them, including the mechanism of action for adjuvants such as alum. Therefore, current research looks to understand the mechanism of action and create safer and more immunogenic adjuvants to increase the efficacy of our vaccines.

1.3.3 Adjuvants used for influenza vaccines

MF59 and AS03 oil-in-water emulsion adjuvants are the only adjuvants approved for use with influenza vaccines. MF59 adjuvant is included as part of the inactivated influenza virus vaccine administered to infants 0 -2 years old ("Canadian immunization guide chapter on influenza and statement on seasonal influenza vaccine for 2016-2017," 2017). AS03 has only been formulated with H5N1 vaccines stockpiled in case of a pandemic outbreak (Sun et al., 2017). Since MF59 and AS03 are both oil-in-water emulsions they have a similar mechanism of action. Both of these adjuvants enhance the local immune response by increasing the uptake of the paired antigen as well as increase the presentation of the antigen on antigen presenting cells (Galson, Truck, Kelly, & van der Most, 2016).

When looking at the influenza vaccines in development and the discussion of a universal vaccine, adjuvants are always part of the equation. Although the two currently used adjuvants are effective in increasing protective antibody titres against influenza antigens it is still important to strive for more effective adjuvants. Since influenza is an RNA virus it makes sense to develop adjuvants, which target the host's defense systems against these viruses, which is the goal of this project. Recently toll-like receptor agonists have become a target for adjuvant development due to their role in host defence (Alving et al., 2012). Therefore, it makes sense to look at other host defense pathways, which are specific to the virus of interest. Influenza A virus is an RNA virus, which is sensed by retinoic acid-inducible gene I-like receptors in the cytoplasm therefore, the agonists for these receptors may be optimal adjuvants for RNA viruses.

1.4 Retinoic acid-inducible gene I (RIG-I)

1.4.1 RIG-I structure

Host recognition and defence against invading pathogens relies pattern recognition receptors (PRR) (Lassig & Hopfner, 2017; Patel & Garcia-Sastre, 2014; X. X. Xu et al., 2017). The activation of PRRs is important in both the innate immune response, which eliminates the pathogen at the site of infection, and the adaptive immune response, which induces long term immunity via antibodies (Patel & Garcia-Sastre, 2014). Retinoic acid-inducible gene I-like receptors (RLRs) are cytosolic viral RNA sensing receptors that are part of the vast superfamily 2 (SF2), which are nucleic acid-dependent NTPases (Lassig & Hopfner, 2017). The RLR family consists of three different proteins which are; retinoic acid-inducible gene I (RIG-I), melanoma differentiation-associated gene 5 (MDA5), and laboratory of genetics and physiology 2 (LGP2) (Lassig & Hopfner, 2017).

RIG-I is a cytosolic receptor that recognizes blunt ended short double stranded RNAs (dsRNA) with a 5' triphosphate moiety, leading to interferon (IFN)-β induction (Hornung et al., 2006; Weber, 2015; X. X. Xu et al., 2017). There are three major domains in the RIG-I structure. They are the n-terminal tandem caspase recruitment domain (CARD), DExD/H-box helicase domain, and the c-terminal domain (CTD) attached by a flexible linker region (Kato et al., 2006; Weber, 2015). In the cell RIG-I can be found in two different states, activated or auto-inhibited (Figure 1). The auto-inhibited state occurs in uninfected cells, the CARD domain is bound tightly to the helicase domain and the CTD is free to scan the cytoplasm for ligands (Weber, 2015). Upon binding of the CTD to a ligand, RIG-I goes through a conformational change to an active or signaling state. In this state both the CTD and helicase domain bind the ligand, due to the helicase binding the ligand, the CARD domain is freed from inhibition (Weber, 2015). Once free

the CARD domain acts as a signal transducer leading to translocation to the outer mitochondrial membrane to interact with the adapter protein mitochondrial antiviral signaling (MAVS), which is also known as VISA, CARDIF or IPSI (Kawai et al., 2005; Meylan et al., 2005; Seth, Sun, Ea, & Chen, 2005; L. G. Xu et al., 2005).

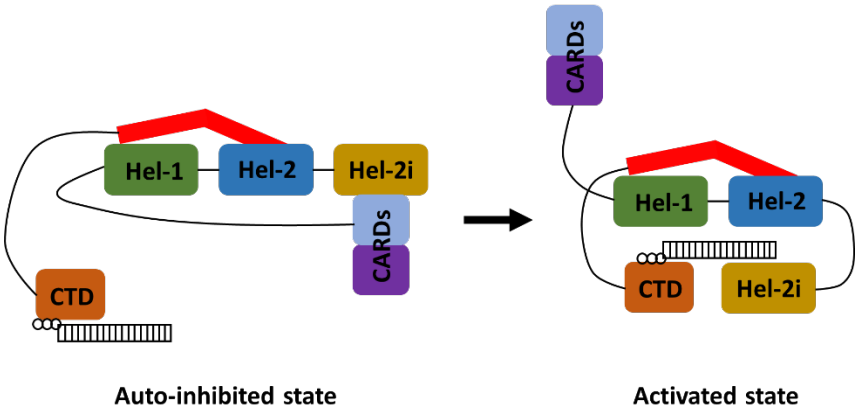

Figure 1: Schematic of RIG-I in both the auto-inhibited state and activated state after binding an agonist.

1.4.2 RIG-I pathway

In the host cell RNA containing a 5' triphosphate moiety can be from two sources, the first being produced by host RNA polymerases and the second from viruses (Patel & Garcia-Sastre, 2014). However, for 5' triphosphate RNAs being produced by the host, the RNA polymerases either modify the 5' end (RNA polymerases I and III) or cap the 5' end (polymerase II) to no longer expose the 5' triphosphate moiety. In comparison, viral RNA does not undergo any modifications leaving the exposed 5' triphosphate end exposed for RIG-I to sense (Patel & Garcia-Sastre, 2014).

When the CTD of RIG-I comes in contact with the blunt end 5' triphosphate RNA the structure goes through a conformational change to the signaling state unmasking the previously bound CARD domain (Kolakofsky, Kowalinski, & Cusack, 2012). The released CARD domain is then ubiquitinated by Riplet (Oshiumi, Matsumoto, Hatakeyama, & Seya, 2009) and E3 ligase

TRIM25 (Gack et al., 2007) forming an active tetrameric unit. Once a RIG-I molecule bound to a ligand is ubiquitinated it forms a tetramer structure with two other ubiquitinated RIG-I molecules creating a lock-washer shaped structure (Peisley, Wu, Xu, Chen, & Hur, 2014), which once translocated to the outer mitochondrial wall is ready to interact with MAVS (Patel & Garcia-Sastre, 2014).

The interaction of the RIG-I tetramer with MAVS leads to the aggregation and redistribution of MAVS on the mitochondria leading to the formation of prion-like fibers, indicating activation (S. Liu et al., 2015; Patel & Garcia-Sastre, 2014). The E3 ligase family TRAF then ubiguitinates active MAVS leading to the activation of IKK and TBK1 kinases, which in turn phosphorylate MAVS (S. Liu et al., 2015). Once phosphorylated MAVS binds to interferon regulatory factor 3 (IRF3), due to this association IRF3 is brought in close contact with TBK1 and is subsequently phosphorylated. After phosphorylation IRF3 disassociates from MAVS and forms a dimer with another phosphorylated IRF3 through positively charged surfaces (S. Liu et al., 2015). The newly formed dimer can then relocate to the nucleus of the cell where it functions alongside nuclear factor (NF)-κB to turn on the expression of type-I interferons and other inflammatory cytokines (S. Liu et al., 2015).

1.5 Hypotheses and objectives

This project focuses on RNA-LZ-1, which is a small RNA molecule that has a strong binding affinity for the cytosolic receptor RIG-I. The main goals are to characterize cytokines, chemokines, and interferons induced by RNA-LZ-1 both *in vitro* and *in vivo*, as well as evaluate its potential as an adjuvant when formulated with an antigen against influenza A infection. We hypothesize that due to RNA-LZ-1's binding affinity for RIG-I it will trigger a robust immune

response and a fortified adaptive response when used as an adjuvant. In order to address our hypothesis, we have separated our experiments into three clear objectives, which are as follows:

1. To determine cytokines and interferons induced by RNA-LZ-1 *in vitro,*
2. To determine cytokines, chemokines, and interferons induced by RNA-LZ-1 *in vivo*, and
3. To determine the efficacy of RNA-LZ-1 as a potential adjuvant for influenza A virus *in vivo.*

By addressing these objectives, we will test whether our hypothesis is correct or not. The following chapters discuss the experiments and results obtained for each of the objectives.

Chapter 2 RNA-LZ-1 induced immune response *in vitro*

2.1 Introduction

RNA-LZ-1 is a blunt ended, short double stranded RNA molecule with a 5' triphosphate moiety derived from the 3' and 5' non-coding regions of the influenza A genome (Figure 2).

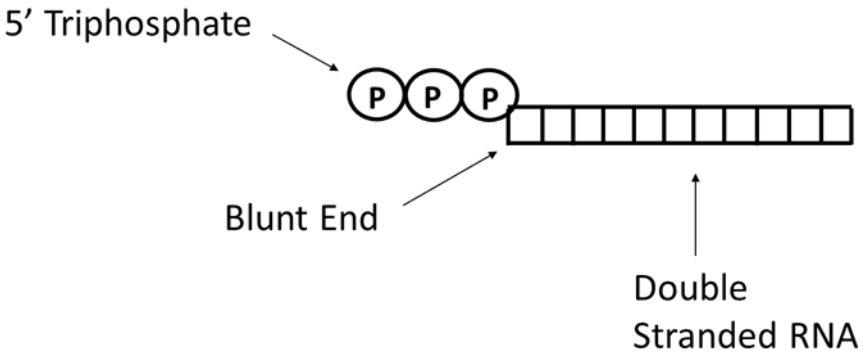

Figure 2: Schematic of RNA-LZ-1, derived from the 3’ and 5’ non-coding regions of the influenza A genome, which is a RIG-I agonist.

Previously in our laboratory RNA-LZ-1 was shown to have a high binding affinity for RIG-I and to stimulate strong interferon response (Liu, Park, Pyo, Liu, & Zhou, 2015). In recent literature, it has been shown that RIG-I agonists have the potential to serve as adjuvants for vaccines against RNA viruses (Beljanski et al., 2015; Martinez-Gil et al., 2013). Since we know that *in vitro* RNA-LZ-1 binds to RIG-I and stimulates interferon promoter activity, we wanted to test this interaction further by showing the induction of type-I interferon (IFN) IFN-β, which is a hallmark of the RIG-I pathway. *In vitro,* we also wanted to show the induction of other inflammatory cytokines. To look into the production of these inflammatory cytokines and interferons we chose to use human cell lines from cell types that can be naturally infected by influenza including human lung epithelial cells and macrophages. The basic outline of this experiment is to transfect RNA-LZ-1 or polyI:C, a known RIG-I agonist, into the cell lines and by collecting the supernatant for protein expression and the cell lysate for RNA extraction, we

can quantify IFN-β levels at both the mRNA and protein level and other cytokines production at the protein level. These data will allow us to gain an overarching view of what is happening upon transfection of RNA-LZ-1. We hypothesize that RNA-LZ-1 will induce similar amounts of IFN-β in comparison to polyI:C, since both are strong RIG-I agonists.

2.2 Materials and methods

2.2.1 Cell lines

THP-1 human monocyte cells were maintained suspensory in RPMI-1640 media (ATCC, 30-2001) containing 10% fetal bovine serum (Gibco, 16000-044), 100 times dilution of penicillin streptavidin (Gibco, 1514163), 55 μM beta-mercaptoethanol (Gibco, 21985-023), and 100 mM sodium pyruvate (Gibco, 11360-070). Cells were plated in 12-well plates at a density of 4×10^5 cells/well and phorbol myristate acetate (PMA) (Sigma-Aldrich, P8139-1mg) was added to differentiate the monocytes into macrophages. A549 human lung epithelial cells were maintained in F-12K media (Gibco, 21127-022) containing 10% fetal bovine serum and 100 times dilution of penicillin streptavidin (Gibco, 15140163). A549 cells were plated in a 12-well plate at a density of 2.5×10^5 cells/well.

2.2.2 RNA-LZ-1 synthesis

T7 *in vitro* transcription, MEGAshortscript kit (Ambion Life Technologies, AM1354), was used to synthesize the RNA-LZ-1. Fifty nanograms of both the T7 promotor primer and the RNA-LZ-1 primer, sequence 5'mGmGCAAAAGCAGGGTACGAATACCCTTGCTTTTG CCTATAGTGAGTCGTATTAAATT-3', were annealed together by heating the mixture up to 95ºC for five minutes and then slowly cooling the mixture to 4ºC. By annealing the primers a template sequence is made, the template is then diluted ten times in RNase free water so that a concentration of 5 pmol/μl is achieved. One microliter was then incubated with T7 enzyme mix,

rNTPs (150 nmol/each), 10 × T7 buffer, and RNase free H_2O overnight at 37ºC. Turbo DNase was then added to the mixture and incubated at 37ºC for 15 minutes. The turbo DNase is added to degrade any remnants of template DNA in the mixture. RNA-LZ-1 was then purified using a mini quick spin column (Sigma, 11814427001). First the column matric needs to be re-suspended by gentle flicking. Next centrifuge the column at 1000 g for 1 minute to remove any residual buffer. The RNA-LZ-1 mixture can then be added to the column and centrifuged for 4 minutes at 1000 g. RNA-LZ-1 was then present in the eluant and a nanodrop2000 (Thermo Scientific) was used to determine the concentration.

2.2.3 Transfection

A549 cells and differentiated THP-1 cells were transfected with 1 µg of either RNA-LZ-1 or low molecular weight (LMW) polyI:C (Invivogen, tlrl-picw). The day after cells were seeded, wells were checked for confluency (60-80%) before being transfected. Opti-MEM (Gibco, 31985-070) was added to two 1.5 ml tubes, 150 µl per tube. In one tube 15 µl of Lipofectamine RNAiMAX (Invitrogen, 13778-150) was added, in the other tube 1 µg of either RNA-LZ-1 or LMW polyI:C was added. The diluted RNA was then added to the diluted Lipofectamine RNAiMAX tube, a 1:1 dilution ratio, and let incubate at room temperature for 30 minutes. After the incubation period the transfection mixture is added drop wise to the designated well. The cells are then incubated with the transfection mixture for ~16 hours at 37°C before media is replaced. Cells are then incubated for another 32 hours, 48 hour total incubation, before supernatant is collected and stored at -80°C and RNA is extracted from the cells.

2.2.4 RNA isolation and real-time quantitative polymerase chain reaction (qPCR)

RNA was extracted from transfected cells using the TRIzol extraction method. After the supernatant was removed from the well 1 ml of TRIzol reagent (Ambion, 15596018) was added

to the cells. The TRIzol was gently pipetted up and down to remove the cells from the bottom of the well and lyse them. After moving the homogenized TRIzol and cell mixture to a 1.5 ml tube the mixture was incubated for 5 minutes at room temperature. Chloroform (Sigma, C2432-500ml) was then added to the TRIzol mixture and the tube was shaken vigorously for 15 seconds and incubated at room temperature for 3 minutes. The sample was then centrifuged for 12,000 g for 15 minutes at 4°C. The aqueous phase, which contains the RNA, was then moved into a new tube and isopropanol (Sigma, 19516-500ml) was added to isolate the RNA. Incubation was 10 minutes at room temperature before centrifuging 12,000 g for 10 minutes at 4°C. The RNA could now be seen visually as a white pellet at the bottom of the tube. To wash the RNA 75% ethanol made in diethylpyrocarbonate (DEPC) containing H_2O (Invitrogen, 46-2224) was used. The sample is vortexed briefly and centrifuged at 7,500 g for 5 minutes at 4°C. The RNA pellet was then air dried for 10 minutes before being re-suspended in RNase free H_2O. Finally, the re-suspended RNA was incubated at 55°C for 15 minutes before determining the concentration using a nanodrop2000 (Thermo Scientific) and being stored at -80°C.

Reverse transcription was done using 500 ng of RNA to make cDNA for qPCR. First the RNA was treated with 100U DNase I (Invitrogen, 18068-015) to degrade any genomic DNA that may still be present in the RNA sample before we convert it back into DNA. The DNase I mixture was incubated at room temperature for 15 minutes and then 25 mM EDTA (Invitrogen, Y02353) was added, aiding in inactivation of DNase I, and the mixture was incubated again at 65°C for 10 minutes. A 10 mM dNTP mix (Invitrogen, 18427-088) and 50 µM of oligo(dT) primer were added to the sample and incubated at 65°C for 5 minutes then moved onto ice for another 2 minutes. The final reverse transcription reaction was then done, 5 × FS buffer (Invitrogen, Y02321), 0.1 M DTT (Invitrogen, Y00147), RNase out (Invitrogen, 10777-019), and

superscript III reverse transcriptase enzyme (Invitrogen, 18080-044) were are all added to the mixture and incubated at 50°C for 1 hour and then heated to 70°C for 15 minutes. The cDNA diluted 10 times in DEPC H_2O was then ready to use for qPCR to detect IFN-β mRNA levels. IFN-β was the gene of interest and GAPDH was used as a housekeeping gene. SYBR green master mix (Applied Biosystems, 4367659) and 10 μM of each primer were added to the designated tubes for qPCR and ran on a real time PCR system (StepOnePlus, Applied Biosystems). Results were quantified using the ΔΔCT method (Lin et al., 2012).

2.2.5 Enzyme-linked immunosorbent assay (ELISA)

The supernatant from the transfected samples was used to detect IFN-β protein levels. A 96-well plate was coated with 0.2 μg/μl of purified anti-human IFN-β (R&D, AF814) in coating buffer (0.015 M $NaCO_3$, 0.035 M $NaHCO_3$ in ddH_2O, pH 9.6) and left at 4°C overnight. The next day the plate was washed four times in 1 × TBST (0.1 M Tris, 0.17 M NaCl, 0.05% Tween 20 in ddH_2O) before being blocked with 1% bovine serum albumen (BSA) (Sigma-Aldrich, A7906-100g) for 1 hour. After the blocking time was completed the plate was washed four times again with 1 × TBST. The standard was then added to the plate, starting at a concentration of 4000 pg of human IFN-β (Temecula California, 92590), and was serially diluted 2-fold down the plate wells A-G with well H being the blank. Supernatant samples were then added in triplicate and the plate was incubated at room temperature for 2 hours. The plate was then washed again before the secondary antibody, biotin labelled rabbit anti-human IFN-β (Abcam, ab84258), was added at a concentration of 1 μg/μl in 1 × TBST containing 0.1% BSA. The secondary antibody was incubated for 1 hour at room temperature. A 1 in 5000 dilution of streptavidin (Jackson Immuno Research Laboratory Inc., 016-050-084) in 1 × TBST containing 0.1% BSA was added to the plate after washing and was incubated at room temperature for another hour. After the

final wash a 1 in 100 dilution of p-nitrophenyl phosphate substrate (PNPP) (Sigma, N3254) in PNPP buffer (1% diethanolamine, 0.5 mM $MgCl_2$ in ddH_2O) was added and colour development was observed before reading the plate.

2.2.6 Human multiplex analysis

A human multiplex assay kit (Invitrogen, LHC0001M) was used to assess multiple immune related cytokine protein levels in the supernatant from transfected THP-1 and A549 cells. Magnetic beads coupled to antibodies of choice cytokines were added to a 96-well plate. Supernatant diluted 1 to 1 in assay diluent was added to the beads in duplicate and incubated for two hours at room temperature. The plate is then washed 3 times before a 10 times dilution of biotinylated detector antibody was added. The detector antibody binds to any available proteins of interest. After a final wash 10 times diluted streptavidin-RPE fluorescent tag in RPE-diluent was added to the beads and incubated for 30 minutes at room temperature in the dark shaking on an orbital shaker. Once the incubation period was over a Bio-Plex 200 system powered by luminex xMAP technology (BioRad) was used to read protein levels.

2.2.7 Statistical analysis

A one-way ANOVA with Tukey's multiple comparisons test was used to statistically analyze all data from this objective using GraphPad Prism software.

2.3 Results

2.3.1 RNA-LZ-1-specific production of interferon (IFN)-β

Induction of IFN-β was measured at both the protein level and mRNA level *in vitro*. RNA-LZ-1 was transfected into both human lung epithelial cells and human macrophages and ELISA and qPCR were used to determine protein levels and mRNA levels, respectively. A549 epithelial cells and THP-1 macrophage cells incubated with RNA-LZ-1 resulted in a significantly

induced amount of IFN-β protein in comparison to the mock, transfection reagent control, and polyI:C groups (Figure 3; $p<0.0001$; $p<0.0001$; $p<0.0001$). In THP-1 human macrophages both RNA-LZ-1 and polyI:C significantly induced IFN-β mRNA fold change in comparison to the mock and transfection reagent control groups ($p<0.0001$) (Figure 4). However, in A549 epithelial cells only polyI:C and not RNA-LZ-1 was able to significantly increase mRNA fold change (Figure 4; $p=0.001$).

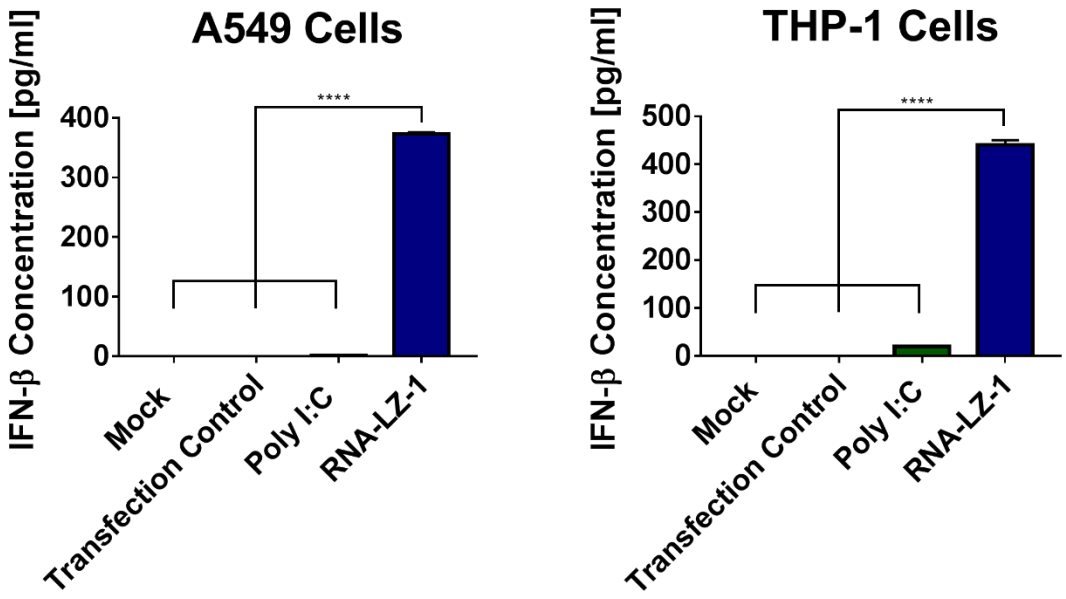

Figure 3: IFN-β protein expression in human epithelial cells and macrophages post-transfection with the RNA-LZ-1. Cells were transfected with 1 µg of either polyI:C, RNA-LZ-1 or an equivalent volume of media with or without the transfection reagent. At 20 hours post-transfection supernatant was collected and used for IFN-β protein analysis with ELISA. Statistical analysis was done using a one-way ANOVA where the p-value was <0.0001.

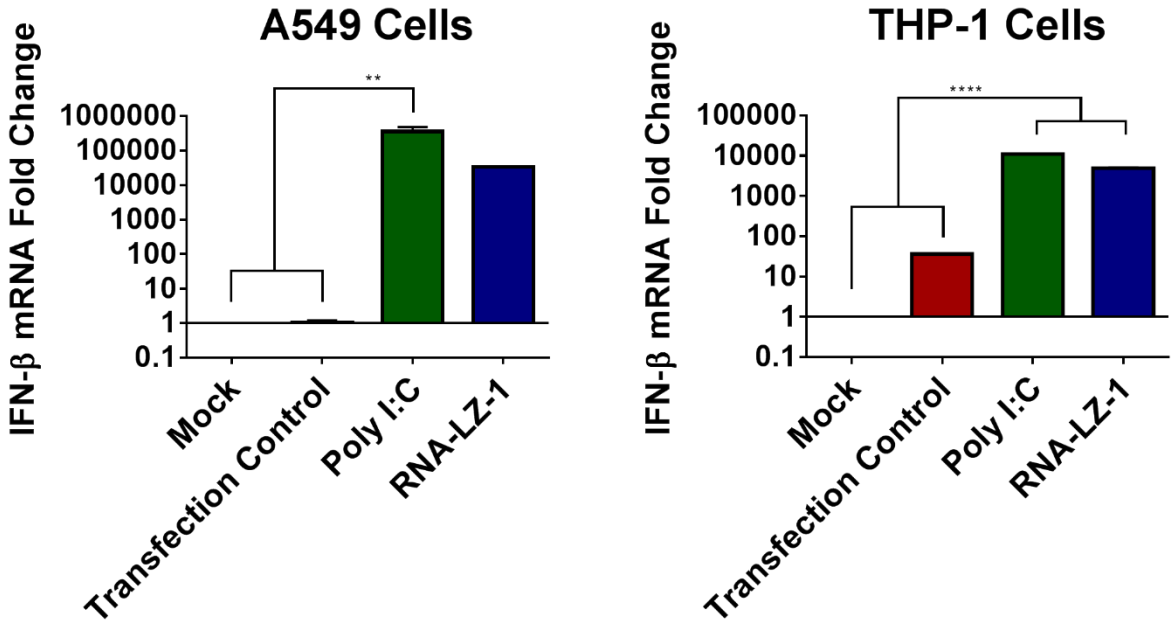

Figure 4: IFN-β mRNA fold change expression was measured in human epithelial cells and macrophages post-transfection with RNA-LZ-1. Cells were transfected with 1 µg of either polyI:C or the RNA-LZ-1 or an equivalent volume with or without transfection reagent. At 20 hours post-transfection cells were collected and RNA was extracted. cDNA was synthesized from 500ng of RNA and used for quantitative real-time PCR. Statistical analysis was done using a one-way ANOVA (** $p= 0.001$, **** $p<0.0001$).

These results match what we were expecting since RNA-LZ-1 has a known affinity for RIG-I binding (G. Liu et al., 2015). At both the protein and mRNA level RNA-LZ-1 was able to induce high amounts of IFN-β compared to the mock and transfection control. Since we confirmed RNA-LZ-1's ability to significantly induce IFN-β production we can move forwards to characterize inflammatory cytokines being produced by RNA-LZ-1 *in vitro*.

2.3.2 RNA-LZ-1-specific production of inflammatory cytokines and chemokines

Once confirming that RNA-LZ-1 does indeed induce the RIG-I pathway, we wanted to look at other cytokines involved in the inflammatory response pathway. A multiplex assay was used to measure the protein levels of multiple cytokines in the supernatant. This method was chosen because in one well you are able to measure the expression of multiple proteins. Significant induction of interleukin (IL)-6 by RNA-LZ-1 in comparison to the mock control was observed in THP-1 (Figure 5A; $p<0.0001$) and in comparison to all the other groups in A549 cells (Figure 5B; $p=0.0005$). IL-8 induction by RNA-LZ-1 was were observed in both cell types as well (Figure 5). In THP-1 cells the transfection reagent control, polyI:C, and RNA-LZ-1 induced IL-8 in comparison to mock (Figure 5A; $p<0.0001$). Whereas in A549 RNA-LZ-1 induced significant levels of IL-8 in comparison to all the other treatment groups (Figure 5B; $p<0.0001$). High levels of IL-8 were observed in all groups in the THP-1 cells (Figure 5A), this has been shown to be due to IL-8 containing archetypal AU-rich elements in its 3'-untranslated regions, which keep the mRNA abundant and stable in human macrophages (Mahmoud et al., 2014). In THP-1 macrophages a slight induction of IL-1β was observed by RNA-LZ-1 compared to the mock group (Figure 5A; $p=0.05$). Neither polyI:C or the transfection control induced IL-1β levels compared to the mock group. IL-4 and TNF-α induction was observed in human macrophages by RNA-LZ-1, however, it was not significant compared to the mock group

(Figure 5A). In the lung epithelial cells there were no other cytokines induced by any of the treatment groups besides IL-6 and IL-8, described above (Figure 5B).

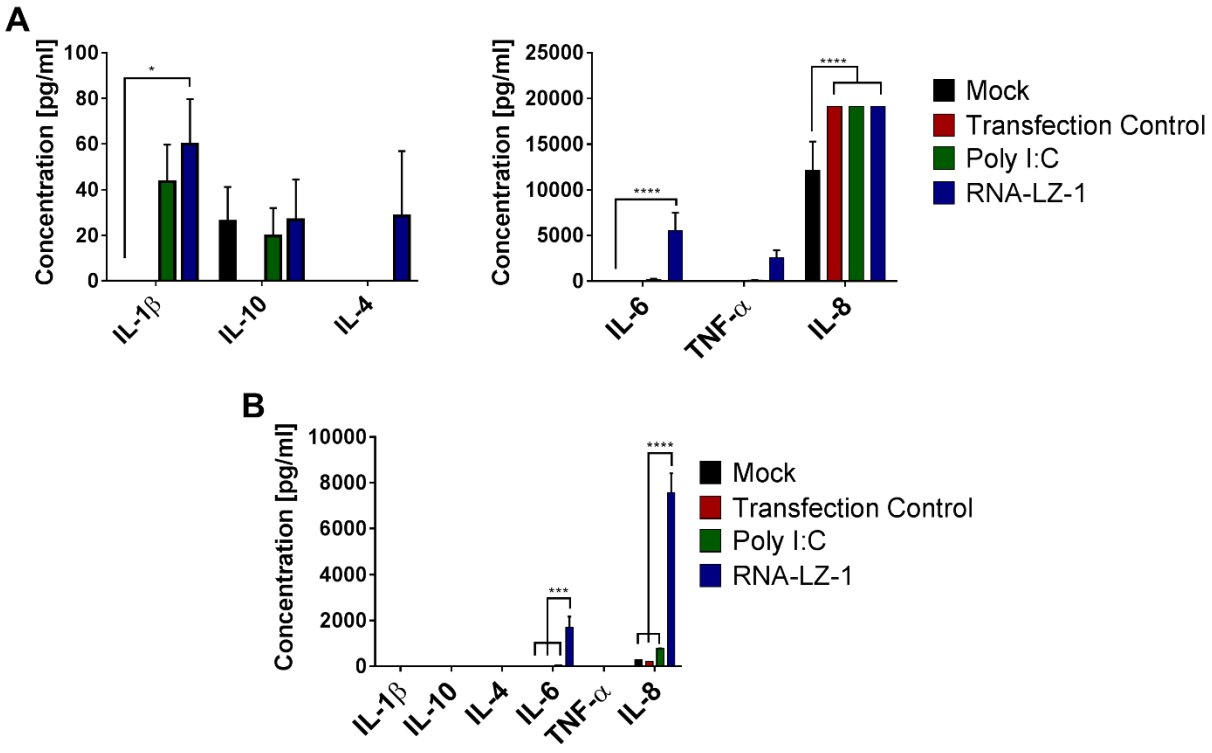

Figure 5: Cytokine protein levels induced by the RNA-LZ-1 *in vitro*. THP-1 cells (A) and A549 cells (B) were transfected with 1 µg of either polyI:C or RNA-LZ-1 or infected with a PR8 NS1 deletion virus at an MOI of 5. Cells were then incubated for 24 hours and supernatant was collected. Supernatant was used for protein analysis by the multiplex assay. Statistical analysis was done using a one-way ANOVA for each cytokine (* p=0.05, *** p=0.0005, **** p=<0.0001).

The differing results in the THP-1 macrophage cell line compared to the A549 epithelial cells was expected, as upon activation of the inflammatory pathway and the expression of interferon regulatory factor-3 (IRF-3) (Thomas, Galligan, Newman, Fish, & Vogel, 2006), downstream of RIG-I activation, a cascade of inflammatory genes are expressed in macrophage cells. These data indicate that RNA-LZ-1 is capable of inducing a downstream inflammatory response due to MAVS signalling through IRF-3. These results strengthen the results of our first objective by showing that RNA-LZ-1 is capable of inducing a broad spectrum of inflammatory cytokines *in vitro*.

2.4 Discussion

RNA-LZ-1 was capable of inducing a wide variety of inflammatory cytokines and interferons *in vitro*. These results strengthened previous data stating that RNA-LZ-1 is a strong RIG-I ligand (G. Liu et al., 2015). In comparison to polyI:C, which is a known RIG-I ligand (Kato et al., 2008), RNA-LZ-1 was able to produce higher protein levels of IFN-β and inflammatory cytokines *in vivo* in comparison to the mock control group. PolyI:C is not only a RIG-I agonist it is also an agonist of toll-like receptor 3 (Lee et al., 2016). In THP-1 human macrophages toll-like receptor 3 is not present (Carpenter, Wochal, Dunne, & O'Neill, 2011), therefore, polyI:C is only activating one of its compatible pathways, which could account for the non-significant increase in levels of inflammatory proteins observed in the polyI:C group (Figure 5A). All cytokines produced were pro-inflammatory and indicative of a Th1 immune response (Lyke et al., 2004). As mentioned above an explanation for why the induction of these cytokines was more prevalent in the THP-1 cells is because macrophages are the dominant cell type producing these cytokines downstream of IRF3 signaling (Thomas et al., 2006). The results from this objective give us solid evidence that RNA-LZ-1 could act as an adjuvant, due to the robust

immune response seen *in vitro*. Since we have observed this inflammatory response *in vitro* the next logical step is to look at the effects of RNA-LZ-1 *in vivo*.

Chapter 3 Transitioning RNA-LZ-1 from an *in vitro* model to an *in vivo* model

3.1 Rational

RNA-LZ-1 was capable of inducing significant amounts of IFN-β in both human macrophages and lung epithelial cells. An increase in inflammatory cytokine protein levels was also observed in both cell types. This observation of inflammatory cytokines and interferon induction *in vitro* was also observed in another study working with a RIG-I agonist derived from vesicular stomatitis virus, M8 (Chiang et al., 2015). M8 was also proven to provide protection against a paired influenza A antigen in a mouse model (Chiang et al., 2015). Therefore, since RNA-LZ-1 and M8 should be activating the same pathway we want to characterize an *in vivo* model, which will test RNA-LZ-1 as a potential adjuvant. To properly develop an *in vivo* mouse model, we need to first determine the optimal dose and characterize the immune response gene profile. Chapter 4 will address the development of a mouse model for RNA-LZ-1 injection.

Chapter 4 RNA-LZ-1 induced immune response *in vivo*

4.1 Introduction

In order to characterize how RNA-LZ-1 induces an inflammatory response as an adjuvant, it is important to understand the immune response being elicited by RNA-LZ-1 alone. *In vitro* we have shown that RNA-LZ-1 binds to the cytosolic sensor RIG-I (G. Liu et al., 2015) and activates the downstream inflammatory response, including induction of IFN-β and the NF-κB pathway, therefore, we know at least part of the mechanism of inflammatory induction by RNA-LZ-1. Knowing the mechanism by which a potential adjuvant acts is essential knowledge that adds to the safety profile of RNA-LZ-1 and justifies moving forwards with testing *in vivo*. Moving into a mouse animal model we first wanted to determine the optimal dose of RNA-LZ-1 which we expect will be different than that used in the cell culture studies. The doses used were chosen based on previous literature working with small RNA molecules, which were RIG-I ligands (Goulet et al., 2013). The dosage trial revealed that the optimal dose was 5 μg of RNA-LZ-1 based on the broad induction of inflammatory cytokines, chemokines, and interferons (Figure 6). After the correct dose was determined we wanted to know at what time points inflammatory cytokines, chemokine, and interferons are upregulated which in turn would establish the length of time which RNA-LZ-1 induces a local immune response. In this objective, we also looked at the kinetics of a previously tested adjuvant, VIDO's triple adjuvant, this was to compare the immune responses between a proven adjuvant and RNA-LZ-1. We hypothesize for this objective that RNA-LZ-1 will produce a robust immune response *in vivo*.

4.2 Materials and methods

4.2.1 Formulation of RNA-LZ-1 injection

RNA-LZ-1 was paired with the *in vivo* transfection reagent *in vivo*-jetPEI (Polyplus transfection, 201-106) for all injections. The transfection reagents mediates an efficient delivery of DNA, RNA, etc. to a wide range of animal tissues. Based on previous literature (Beljanski et al., 2015) the amounts of 1, 2.5, and 5 μg of RNA-LZ-1 were chosen to be used in the dosage trial. When complexing RNA-LZ-1 with *in vivo*-jetPEI the first thing to consider is the N/P ratio, which is defined as the ionic balance within the complex and is the number of nitrogen residues in *in vivo*-jetPEI per nucleic acid phosphate. The manufacturer suggests an N/P value between 6 and 8, so we used an N/P ratio of 8 for all studies. The amount of *in vivo*-jetPEI can be calculated using a simple equation provided in the protocol booklet:

$$\mu l\ of\ in\ vivo - jetPEI = \frac{(\mu g\ RNA \times 3)\left(\frac{N}{P} ratio\right)}{150}$$

Equation 1: Equation to determine the amount of *in vivo*-jetPEI needed for a specified amount of RNA. The N/P ratio used was 8. This equation is from the *in vivo*-jetPEI protocol booklet provided with the reagent from Polyplus transfection.

The specified RNA-LZ-1 concentration was added into half the injection volume of double distilled H_2O and 5% glucose, provided in the kit. The calculated amount of *in vivo*-jetPEI was added to the other half of the injection volume. Each tube is briefly vortexed and then the diluted *in vivo*-jetPEI is added to the RNA-LZ-1 tube and vortexed gently before being incubated at room temperature for 15 minutes. The injection is now complexed and is stable at 4°C for up to 7 days according to the manufacturer (Polyplus transfection).

4.2.2 Ethics statement

I*n vivo* studies were performed at the Vaccine and Infectious Disease Organization – International Vaccine Center (VIDO-InterVac), University of Saskatchewan. All procedures and animal care complied with the ethical guidelines of the Canadian Council of Animal Care and the University of Saskatchewan Committee on Animal Care and Supply. The following experiments were approved by the University of Saskatchewan Animal Ethics Board.

4.2.3 Dosage mouse trial

Naïve female BALB/c mice (Charles River) at six weeks of age were used in this study. Animals were randomly assigned into six groups (N=5). RNA-LZ-1 was injected at three different doses (1, 2.5, and 5 μg) alongside *in vivo*-jetPEI transfection reagent (described above). Each dose of RNA-LZ-1 had its own control group consisting of the specified volume of *in vivo*-jetPEI in double distilled H_2O with 5% glucose. Mice were allowed to acclimatize for 1 week before receiving their specific injection, which was given intra-muscularly into the semi-membranous muscle with 25 μl of injection per leg. The intra-muscular injection route was chosen for all animal trials as influenza vaccines are given intra-muscularly in humans. After 24 hours mice were sacrificed and the injection site, semi-membranous muscle, was removed.

4.2.4 Dual Luciferase assay

Human embryonic kidney cells (HEK293T) were plated in a 24-well plate at a density of 2×10^5 cells per well the night before the assay. The next day cells were transfected with plasmids expressing RIG-I, IFN-β promoter firefly luciferase, and renilla luciferase using TransIT-LTI transfection reagent (Mirus, MIR2300). Six hours post-transfection the cells were transfected with the RNA-LZ-1 or polyI:C, using RNAiMAX transfection reagent. Twenty-four hours post-transfection cells were lysed using passive lysis buffer. A one to one ration of LarII

(Promega, E1960) to sample was mixed together and the firefly luciferase concentration was read. Next the same volume of Stop and Glo (Promega, E1960) was added to quench the firefly luciferase and activate the renilla luciferase. Then the ratio between the two luminescence was determined.

4.2.5 Formulation of VIDO's triple adjuvant and the modified triple adjuvant

VIDO's triple adjuvant was formulated as described below. The polyI:C (Invivogen, tlrl-picw), host defence peptide (peptide) (CPC Scientific Inc., 818360), and polyphosphazene EP3 (VIDO EP3 Lot A) were added at a 1:2:1 ratio respectively. PolyI:C (10 µg/mouse) and peptide (20 µg/mouse) were complexed together by incubating the mixture for 15 minutes with PBS pH 7.4 (Gibco, 10010-031) at room temperature. The light sensitive polyphosphazene EP3 (10 µg/mouse) was then added and the mixture and incubated for another 15 minutes at room temperature. The adjuvant mixture was then stored in the dark at 4°C until needed for injection. In the case of the modified triple adjuvant the same procedure is followed except 10 µg per mouse of RNA-LZ-1 replaced polyI:C in the formulation.

4.2.6 Kinetics mouse trial

Naïve, 6-week old female BALB/c mice were split into treatment and control groups (N=5) for each of the following time points 3, 6, 24, 48, and 72 hours post-injection. On day 0 mice were injected intra-muscularly into the semi-membranous muscle, 25 µl per leg, with either 5 µg of RNA-LZ-1 complexed with *in vivo*-jetPEI, *in vivo*-jetPEI control, VIDO triple adjuvant, modified triple adjuvant, or PBS. At the designated time points each group of mice were sacrificed and the injection site tissue was collected.

4.2.7 RNA isolation from injection site

RNA was extracted from the injection site tissue using the TRIzol extraction method. The semi-membranous muscle had any excess fat trimmed from it and was then cut into smaller pieces before being placed in a bead beater tube. One milliliter of TRIzol reagent was added to the tube then the tissue was homogenized in a bead beater (Biospec Products) for approximately 16 seconds at speed setting 48. After homogenization samples were incubated for 5 minutes at room temperature, allowing the dissociation of nucleoprotein complex. Chloroform was then added to the sample and shaken vigorously for 15 seconds before being incubated for 2 minutes at room temperature. Samples were then centrifuged at 12,000 g for 15 minutes at 4°C. The RNA, which is located in the aqueous phase, was moved to a new tube where isopropanol was added to precipitate the RNA. The isopropanol and aqueous phase mixture was incubated for 10 minutes at room temperature and then centrifuged at 12,000 g for 10 minutes at 4°C. A white pellet, the RNA, should be visible after centrifugation. The RNA pellet was then washed with 75% ethanol by vortexing the sample briefly before centrifuging 7,500 g for 5 minutes at 4°C. Discarding the wash the pellet was allowed to air dry for 10 minutes before being re-suspended with RNase-free water. Once re-suspended the RNA was heated to 55°C for 15 minutes. The concentrations of the samples were then determined using a nanodrop2000 (Thermo Scientific) and stored at -80°C.

4.2.8 Real-time quantitative PCR

cDNA, derived from 500ng of extracted RNA from the animal trials, was used as template for qPCR. Samples were run in triplicate against twenty different cytokines, chemokines, and interferons to test for mRNA expression levels. Three different housekeeping genes, GAPDH, β-actin, and HPRT, were run as internal controls. The most consistent

housekeeping gene for all samples was used as the control. Primers used in both trial are available in the appendix.

4.2.9 Statistical analysis

Statistical analysis was performed using a one way or two way ANOVA in GraphPad Prism software.

4.3 Results

4.3.1 Optimal dosage of the RNA-LZ-1 *in vivo*

For our dosage trial, we selected RNA-LZ-1 concentrations, 1 μg, 2.5 μg, and 3 μg based on a literature search on RIG-I agonists being tested *in vivo*. Animals were injected intra-muscularly into the semi-membranous muscle and sacrificed 24 hours post-injection. The injection site tissue and serum (data not shown) were then analyzed for cytokine, chemokine, and interferon response. In the serum, there was no detection of any cytokine proteins of interest (data not shown). However, we were able to observe gene activation of inflammatory cytokines and interferons for RNA-LZ-1.

Overall there was an increase in gene activation of cytokines and chemokines in four different functional areas. The first area comprised of an increase in interferon activity (Figure 6 B and C). Only the 5 μg concentration of RNA-LZ-1 was able to induce significant fold change in comparison to the control group, the other concentrations tested were comparable to that of the control group (Figure 6 B and C) ($p<0.0001$; $p<0.0001$). The induction of interferons are important to observe as they are the hallmark of activation by the RIG-I pathway. Secondly activation of genes responsible for T-cell and B-cell maturation and differentiation was observed (Figure 6 D and E). IL-12β for instance plays an important role in sustaining sufficient numbers of effector and memory Th1 cells, which are essential for mediating long term memory (Stobie et

al., 2000). For IL-12α and β only the 5 μg concentration induced a significant up-regulation of mRNA, like the interferons the other two concentrations were similar to background levels observed in the mock groups (Figure 6 D and E) ($p<0.0001$; $p<0.0001$). However, for CCL3 (Figure 6H) there was a significant induction of fold change for both the 1 μg and 5 μg concentrations ($p=0.001$; $p=0.0005$), with only the 2.5 μg concentration reflecting background levels. We would have expected to see a dose dependency for CCL3 (Figure 6H) since there was induction at the high and low concentrations, however, that was not the case. The third area with increased activity surrounded chemokines involved in inflammatory cell response, including the recruitment of neutrophils and eosinophils (Figure 6 G, H, and I). CCL2 (Figure 6G; $p<0.0001$) and CCL5 (Figure 6I; $p<0.0001$) saw increased fold change at the 5 μg concentration but not at the 1 or 2.5 μg concentrations. This is crucial to observe as inflammatory cell recruitment is needed to mount an effective immune response against incoming pathogens. Inflammatory cytokine induction was the last area in which gene activation was observed (Figure 6F; $p<0.0001$), IL-6 induction was only observed for the 5 μg dose. For this trial we also looked at gene activation of the anti-inflammatory cytokine IL-10 as a negative control (Figure 6A), like expected there was no upregulation of this gene by any of the RNA-LZ-1 concentrations. After comparing the upregulation of genes involved in the inflammatory response the RNA-LZ-1 concentration of 5 μg had the broadest effect *in vivo*. Moving forwards the 5 μg concentration will be used to explore the kinetics of RNA-LZ-1.

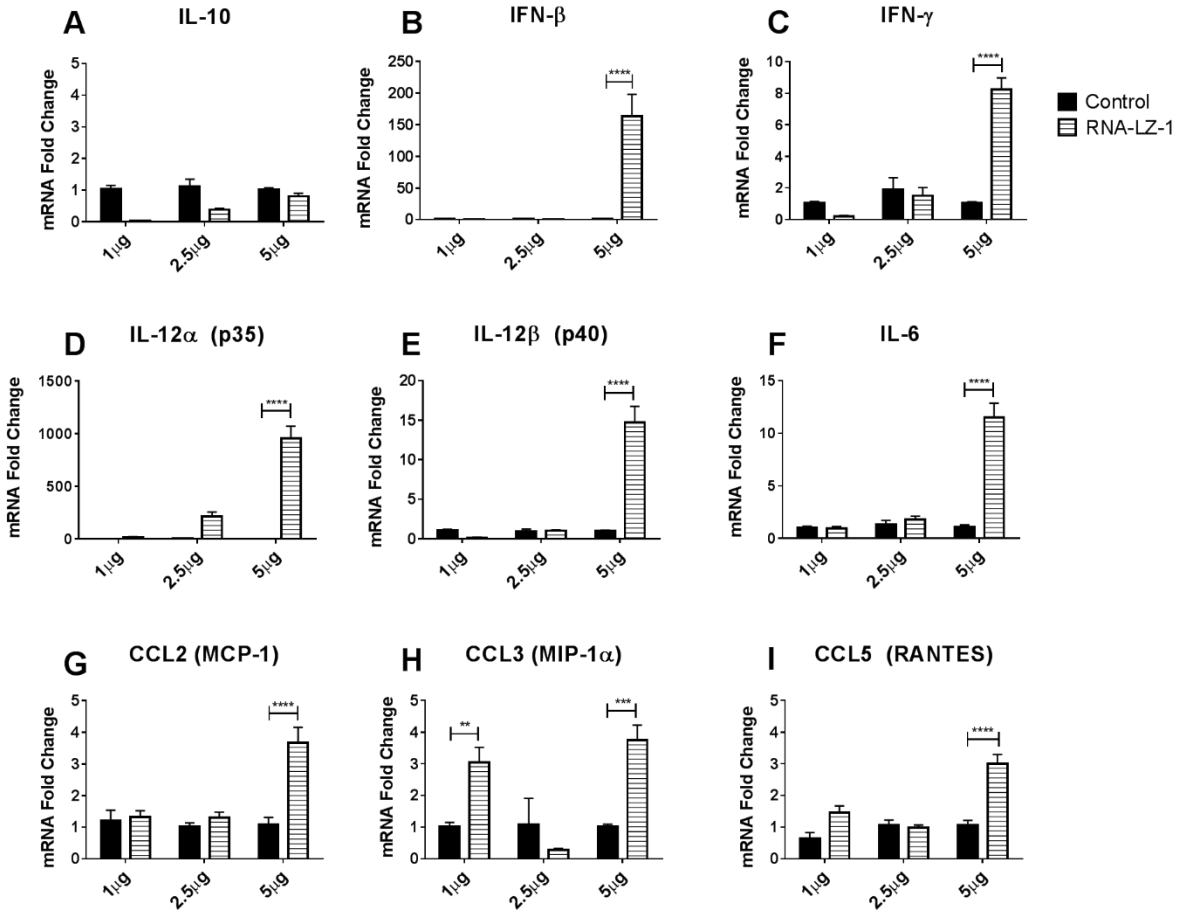

Figure 6: Cytokine and chemokine induction due to RNA-LZ-1. Six-week-old female BALB/c mice were intramuscularly injected with three different doses (1 μg, 2.5 μg, and 5 μg) of RNA-LZ-1. Twenty-four hours post-injection mice were euthanized and the semi-membranous muscle from both hind legs were collected. Total RNA was extracted from the semi-membranous muscle using the TRIzol method. 500 ng of total RNA was used for reverse transcription into cDNA by the oligo(dT) primer. Cytokine and chemokine expression levels were detected using real-time PCR with gene-specific primers. The mRNA fold change was determined using the ΔΔCT method and normalized against the CT values of the housekeeping gene GAPDH. Statistical analysis was done using a two-way ANOVA for each cytokine (* p=0.05, ** p0.001, *** p=0.0005, **** p<0.0001).

4.3.2 Kinetics of immune response genes induced by the RNA-LZ-1

Now that we have determined the optimal dose of RNA-LZ-1 *in vivo*, 5 μg, we decided to look at the immune response elicited at other time points. The first-time point trial we did looked at the effects of RNA-LZ-1 at 24, 48 and 72 hours post-injection. Cytokine and chemokine analysis was done using quantitative real-time PCR. Unlike what we were expecting to observe, RNA-LZ-1 did not appear to activate any of the genes examined at both 48 and 72 hours post-infection. There was no upregulation of IFN-β, IFN-ɣ, or IL-1β genes (data not shown) and no significant gene activation of either IL-12α (Figure 7A) or IL-6 (Figure 7B), which were highly up-regulated in the previous dosage trial at 24 hours post-injection (Figure 7).

The results of the second mouse trial were unexpected compared to the initial dosage trial, leading us to question whether RNA-LZ-1 was still biologically functional or if the effects of RNA-LZ-1 dissipate by these later time points. To test whether RNA-LZ-1 was still functional an IFN-β dual luciferase assay was done. RNA-LZ-1 was transfected into HEK293T cells at both 200 ng and 500 ng concentrations and polyI:C transfected at the same concentrations was used as a positive control. RIG-I was transfected in order to see the IFN response, as HEK293T cells have low levels of endogenous RIG-I. In addition green fluorescent protein (GFP) was transfected as a control for the transfection of RIG-I in order to show that RNA-LZ-1 is RIG-I dependent (Figure 8). RNA-LZ-1 and polyI:C increased in a dose dependent manor compared to the control group (Figure 8). The dual luciferase assay showed us that RNA-LZ-1 was still biologically functional and that even after long term storage at -80°C the integrity of RNA-LZ-1 is not compromised. Based on the fact that RNA-LZ-1 maintained its biological functionality the results observed in Figure 6 can be attributed to the dissipation of the immune response induced by RNA-LZ-1 at these later time points.

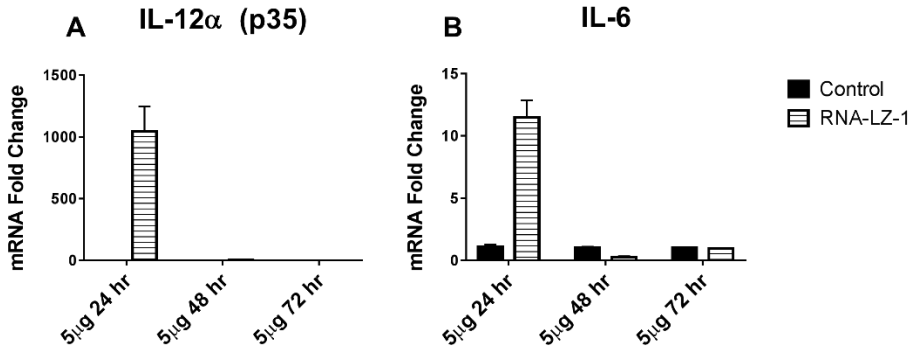

Figure 7: Comparison of the RNA-LZ-1 gene activation at 24, 48, and 72 hours post-injection. Six-week-old female BALB/c mice were injected with either RNA-LZ-1 or the control intra-muscularly into the semi-membranous muscle. Injection site tissue was harvested at designated time points. RNA was extracted from the tissue and 500 ng was used to generate cDNA for real-time qPCR. The mRNA fold change was determined using the ΔΔCT method and normalized against the CT values of the housekeeping gene GAPDH.

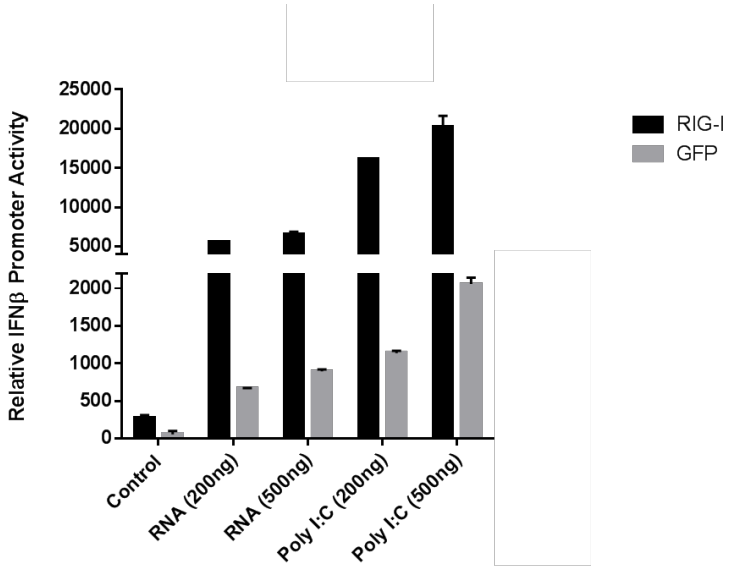

Figure 8: IFN-β induction due to RNA-LZ-1 is dependent upon the presence of RIG-I. RNA-LZ-1 and polyI:C were transfected at a concentration of either 200ng or 500ng with or without RIG-I in A549 cells. IFN-β production was measured using the INF-β dual luciferase assay, where renilla luciferase acts as an internal control. This showed that the production of IFN-β by RNA-LZ-1 and polyI:C is both RIG-I and dose dependent.

The next time points we chose to look at were 3, 6, and 24 hours post-injection. This data provided two patterns of gene up-regulation (Figure 9). The first being highly up-regulated at the earliest time point and slowly dissipating towards 24 hours (Figure 9B) and the second being a peak at the middle time point and low up-regulation at the early and late time points (Figure 9A, C-L). This trial resulted in a wider up-regulation of inflammatory genes than initially observed in the dosage trial, which only looked at 24 hours post-injection. This included the up-regulation of type-I IFNs, IFN-β (Figure 9B; $p=0.0005$) which had significant levels of induction as early as 3 hours post-injection and IFN-α (Figure 9A; $p<0.0001$) which was not observed in the dosage trial as it is expressed at early time points with a significant increase of fold change at 6 hours post-injection. Type-II interferon IFN-ɣ (Figure 9C; $p=0.05$) was also up-regulated at 6 hours post-injection. At early time points we were also able to observe an increase in gene activity related to immune cell recruitment (Figure 9 H-L), indicating that RNA-LZ-1 utilizes immune cells to mount an immune response early on. For MIP-1α (Figure 9H; $p<0.0001$), MCP-1 (Figure 9I; $p=0.001$), RANTES (Figure 9J; $p=0.0005$), and IP-10 (Figure 9L; $p<0.0001$) significant induction of gene regulation was observed at 6 hours post-injection with the up-regulation turned off by 24 hours post-injection. Whereas MIP-2, which is also involved in immune cell recruitment, was up-regulated at 24 hours post-injection (Figure 9K; $p=0.05$). Pro-inflammatory cytokines IL-6 (Figure 9D; $p=0.001$) and IL-18 (Figure 9E; $p<0.0001$) were induced at 6 hours post-injection. The kinetics of IL-10 (Figure 9F; $p=0.001$) the anti-inflammatory cytokine, which is known to turn off the Th1 response (Berger, 2000), was significantly up-regulated at 6 hours post-injection. This induction of IL-10 may be responsible for the dissipation of immune response by 48 hours post-injection. Overall, we showed that RNA-LZ-1 is capable of inducing a potent immune response as early as 3 hours post-injection

with the effects on gene regulation dissipating by 48 hours post-injection. The fact that the immune response lasts only 24 hours could be beneficial in reducing the incidence of cytokine storms, which could be detrimental to the host, when paired with an antigen.

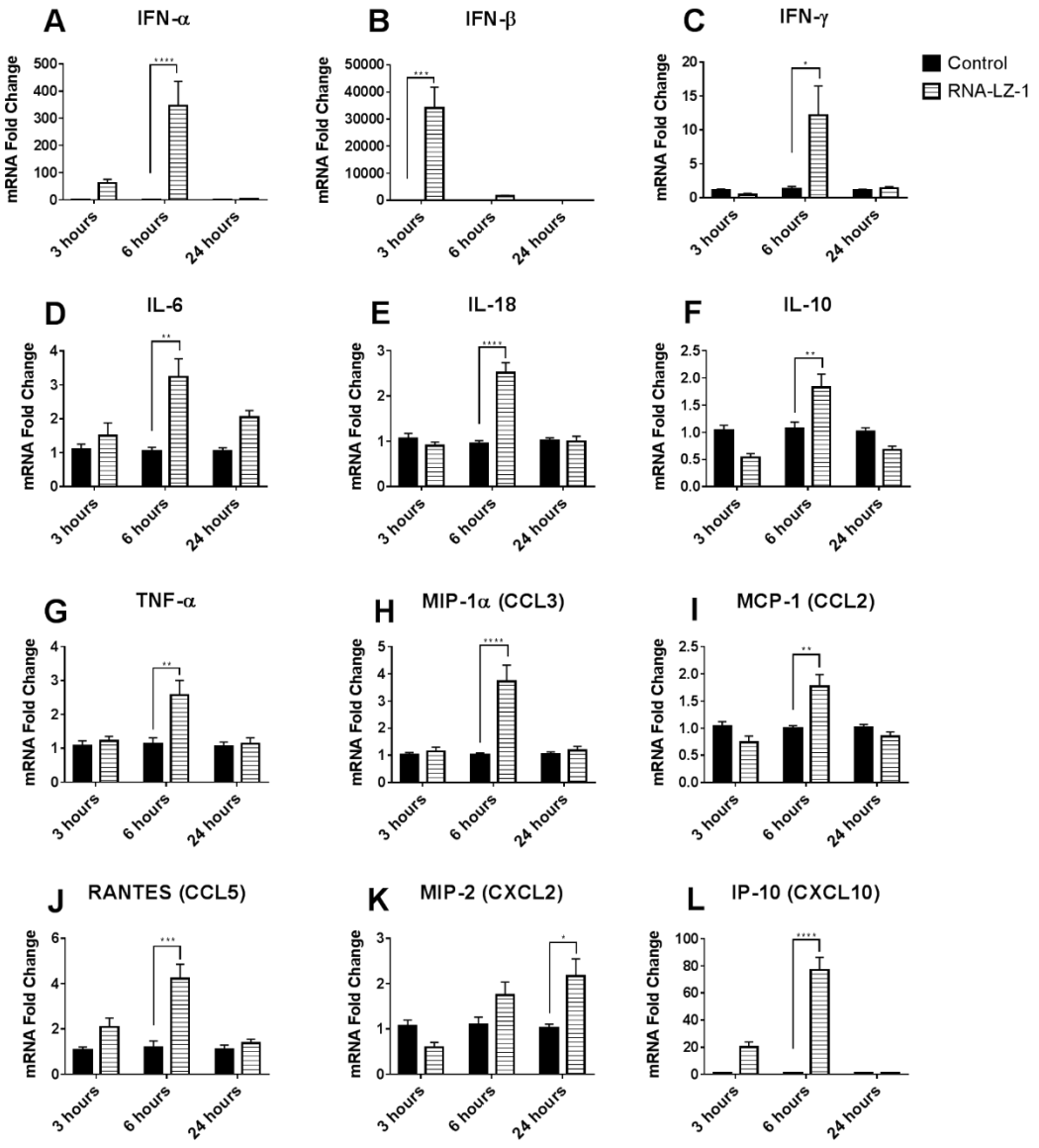

Figure 9: Kinetics of cytokines, chemokines, and interferons induced by RNA-LZ-1 *in vivo*. Six-week-old BALB/c female mice were injected intra-muscularly with either 5 µg of RNA-LZ-1 or the control. At 3, 6, and 24 hours post-injection the injection site tissue was collected. Total RNA was extracted from the semi-membranous muscle using the TRIzol method. 500 ng of total RNA was used for reverse transcription into cDNA by the oligo(dT) primer. Cytokine and chemokine expression levels were detected using real-time PCR with gene-specific primers. The mRNA fold change was determined using the ΔΔCT method and normalized against the CT values of the housekeeping gene GAPDH. Statistical analysis was done using a two-way ANOVA for each cytokine (* p=0.05, ** p= 0.001, *** p=0.0005, **** p<0.0001).

4.3.3 Kinetics of immune response genes induced by VIDO's triple adjuvant and the modified triple adjuvant

Along with looking at the kinetics of RNA-LZ-1 we wanted to compare our results to a proven adjuvant. VIDO's triple adjuvant has been successfully used as an adjuvant previously (Garg et al., 2014). Since polyI:C, a known RIG-I agonist, is a component of the triple adjuvant we also wanted to see the response if RNA-LZ-1 replaced polyI:C in the formulation. We expected that the replacement of polyI:C with RNA-LZ-1, modified triple adjuvant, would lead to a similar or beneficial response in inflammatory gene expression. For this animal trial we only looked at 6 and 24 hours post-injection. Similar with our previous trials the injection site, semi-membranous muscle, was collected and gene response was evaluated using real-time qPCR.

Like we expected VIDO's triple adjuvant was a strong inducer of gene expression for a broad number of inflammatory related cytokines, chemokines, and interferons. However, in comparison to RNA-LZ-1 alone the triple adjuvant tended to up-regulate genes early on and return to basal levels of expression by 24 hours post-injection (Figure 10). Inflammatory cytokine genes IL-12β (Figure 10F; $p<0.0001$), TNF-α (Figure 10G; $p=0.05$), IL-18 (Figure 10H; $p=0.001$), and IL-6 (Figure 10I; $p=0.001$) were all significantly up-regulated at 6 hours post-injection with the fold change returning to basal levels by 24 hours post-injection. However, for IL-1β and IL-12α there was no significant increase in gene expression seen at either time point. The induction of early gene expression was also observed in type-I IFN IFN-α (Figure 10B; $p=0.0005$) and type-II IFN IFN-ɣ (Figure 10A; $p<0.0001$). For type-I IFN IFN-β (Figure 10C; $p=0.001$) a constant significant increase of gene expression in comparison to the mock was observed at both 6 and 24 hours post-injection, it would be interesting to know whether this IFN response dissipates by 48 hours as it did in the case of RNA-LZ-1. Like RNA-LZ-1 VIDO's

triple adjuvant induced a wide variety of chemokines involved in attracting immune cells (Figure 10 J-O). Like the other genes tested the majority of immune cell recruiting genes were significantly up-regulated early on and shut off by 24 hours post-injection. These included KC-GRO (Figure 10J; $p=0.001$), IP-10 (Figure 10L; $p<0.0001$), MCP-1 (Figure 10M; $p<0.0001$), and eotaxin (Figure 10O; $p<0.0001$). For MIP-2 there appeared to be induction at 6 hours post-injection, however, it was not significant (Figure 10K). MIP-1α showed up-regulation at both 6 and 24 hours post-injection although the significance was less at 24 hours (Figure 10N; $p<0.0001$; $p=0.05$). VIDO's triple adjuvant showed to be a potent inducer of inflammatory cytokines, chemokines, and interferons as is expected by a proven adjuvant.

Unlike what was expected, the modified triple adjuvant appeared to have a detrimental effect in comparison to VIDO's triple adjuvant. In this case the addition of RNA-LZ-1 to the peptide and EP3 decreased the gene regulation effect seen when polyI:C is used in the traditional combination. This was surprising since RNA-LZ-1 is capable of inducing high expression alone *in vivo* and in our *in vitro* studies produced more IFN-β and inflammatory cytokines than polyI:C. Only in the case of IL-1β (Figure 10D; $p<0.0001$) and KC-GRO (Figure 10J; $p<0.0001$) at 24 hours post-injection did we see up-regulation of the genes by the modified triple adjuvant.

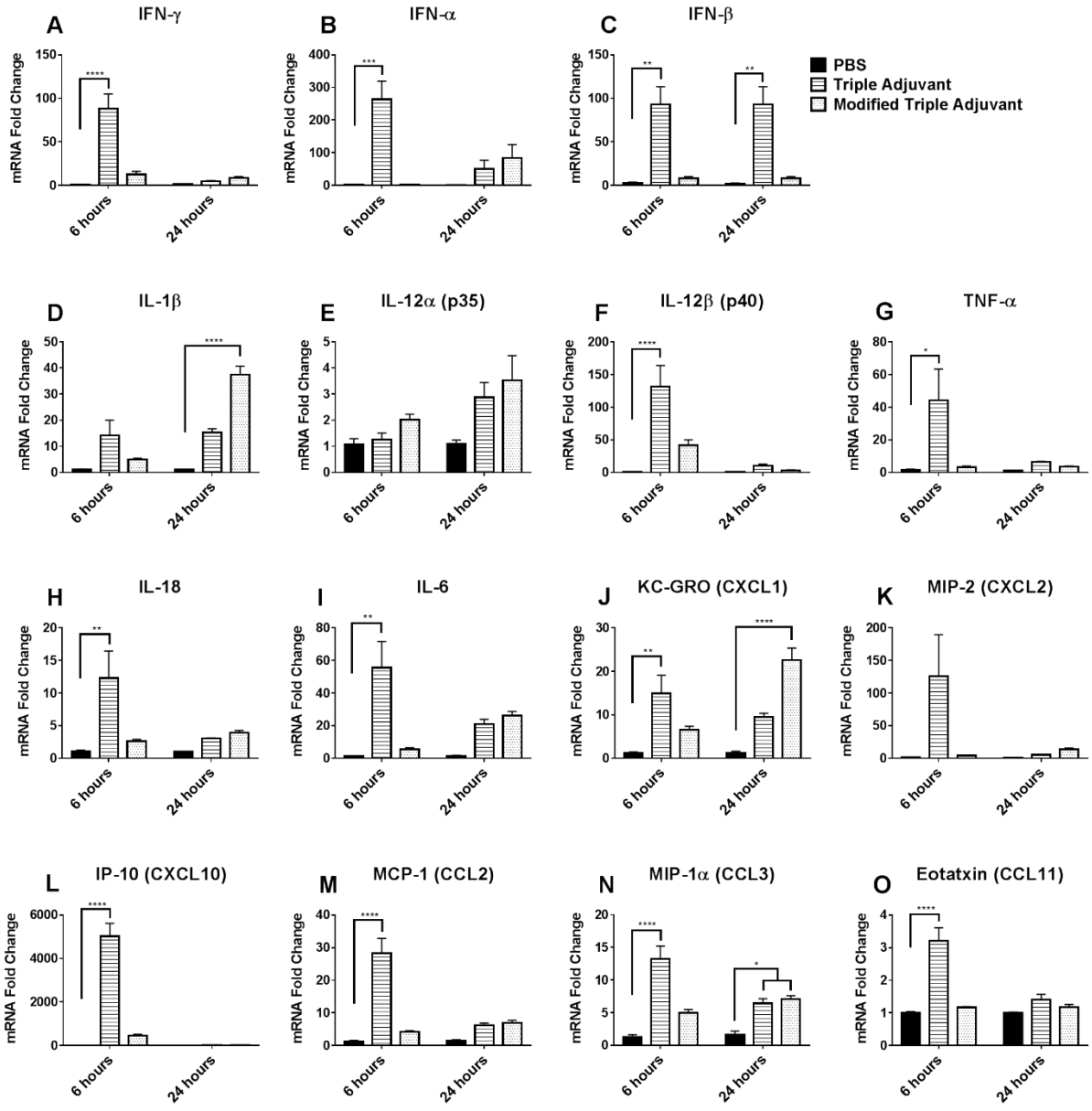

Figure 10: Kinetics of cytokines, chemokines, and interferons induced by the triple adjuvant and modified triple adjuvant *in vivo*. Six-week-old female BALB/c mice were injected intramuscularly with wither the triple adjuvant, the modified triple adjuvant, or phosphate buffered saline. At six and twenty-four hours post-injection mice were euthanized and the semi-membranous muscle from both hind legs was collected. The total RNA was extracted from the tissue using the TRIzol method. 500 ng of total RNA was used to make cDNA using reverse transcription and the oligo(dT) primer. Cytokine, chemokine, and interferon mRNA expression levels were detected using real-time PCR with gene specific primers. The mRNA fold change levels were determined using the ΔΔCT method and normalized against the CT values of the housekeeping gene GAPDH. Statistical analysis was done using a two-way ANOVA for each cytokine (* p=0.05, ** p= 0.001, *** p=0.0005, **** p<0.0001).

4.4 Discussion

RNA-LZ-1 proved to be as potent *in vivo* as it was *in vitro.* Through a dosage trial we determined that a concentration of 5 µg of RNA-LZ-1 was most effective due to its ability to up-regulate a multitude of immune response related genes. Similar to our cell culture work RNA-LZ-1 induced high levels of IFN-β, which is the expected result of a RIG-I agonist. We also determined that the onset of up-regulation of IFN-β occurs early on after injection and slowly dissipates by 48 hours. Type-I IFN IFN-β is not the only interferon up-regulated by RNA-LZ-1, IFN-α another type-I IFN and IFN-ɣ the only type-II IFN were also up-regulated. IFN-α aids in the anti-viral immune response by enhancing the responses of natural killer cells and virus-specific $CD8^+$ T-cells (Cha et al., 2014). IFN-ɣ plays a major role in defining a Th1 immune response along with IL-12 (Schroder, Hertzog, Ravasi, & Hume, 2004), which were up-regulated by RNA-LZ-1 as well. The effects of IFN-ɣ include increasing the efficiency of both MSC class I and II antigen presentation and aiding in the maturation of T-cells, B-cells, and macrophage activation (Schroder et al., 2004). Since IFNs play an important role in innate and adaptive immune response, including antigen presentation, it is important to have an IFN response by adjuvants. VIDO's triple adjuvant also induced a strong IFN response like RNA-LZ-1, however, the modified triple adjuvant was unable to produce up-regulation of any IFN.

Induction of genes related to immune cell recruitment was also observed in both RNA-LZ-1 and VIDO's triple adjuvant treated groups. This is important in mounting an efficient immune response against pathogens by the host. Based on our kinetics studies both RNA-LZ-1 and VIDO's triple adjuvant were capable of inducing a robust local immune response in a mouse model. This allows us to be more confident in our results indicating that RNA-LZ-1 will be an effective adjuvant based on its ability to induce a broad spectrum of cytokines, chemokines, and

interferons. Moving forwards RNA-LZ-1 and VIDO's triple adjuvant will be paired with antigens to evaluate antigen specific immune response.

Chapter 5 RNA-LZ-1 produces a robust immune response indicating potential as an adjuvant

5.1 Rational

RNA-LZ-1 induced significant levels of cytokines, chemokines, and interferons important in immune response at a concentration of 5 μg in an *in vivo* mouse model. When injected intra-muscularly into the semi-membranous muscle up-regulation of immune genes was observed at 3 hours post-injection with the genes returning to basal expression levels by 48 hours post-injection. As a positive control an adjuvant, which has proven to aid in protection against virus challenge, was used as a comparison for the gene profile. RNA-LZ-1 showed similar up-regulation of immune genes to VIDOs triple adjuvant. Therefore, moving forwards both RNA-LZ-1 and VIDOs triple adjuvant will be paired with antigens against avian influenza A viruses. Chapter 6 presents the results from the vaccine trial, which will show whether RNA-LZ-1 has the potential to be an effective adjuvant.

Chapter 6 Inactivated H5N1 and H7N9 vaccines against specified avian influenza A virus strains

6.1 Introduction

Influenza A virus is an important pathogen that causes disease in a wide variety of species, including swine, avian, and human leading to economic loss in the pork and poultry industries and added burden on our health care systems. In order to meet the growing risk of pandemic influenza viruses, there is a demand to create more effective and immunogenic vaccines. Recently, outbreaks of avian influenza viruses in the human population have added to this growing risk. Therefore, strategies to address the demands of higher efficiency, immunogenicity, and safety must be explored. One strategy, which addresses efficiency and immunogenicity, is to explore the addition of an adjuvant to influenza vaccines. Currently the Food and Drug Administration (FDA) has approved an oil in water emulsion (ASO3) adjuvanted H5N1 vaccine for national stock pile in the United States (Cao et al., 2016). This ASO3 adjuvant has also previously been paired with the pandemic H1N1 vaccine, however, children and adults vaccinated with this showed side effects including narcolepsy (Cao et al., 2016). Therefore, there is a need to explore other adjuvant options relating to influenza vaccines specifically.

In our previous objectives, we have shown that RNA-LZ-1 is a strong adjuvant candidate. Since RNA-LZ-1 was able to induce broad spectrum immune response we believe that it will increase the immune response against a paired antigen. In this final objective we look to evaluate the antigen-specific antibody response of animals vaccinated with either the inactivated viruses alone or paired with one of the following adjuvants, RNA-LZ-1 and VIDO's triple adjuvant. Animals were given prime and boost vaccination two weeks apart and sacrificed 10 days post-boost to evaluate the antibody response. Serum was collected prior to each vaccination so that we

could evaluate the difference between a single or double dose of the vaccines. We hypothesize that the addition of RNA-LZ-1 will increase the antigen-specific antibody response in comparison to the inactivated virus alone.

6.2 Materials and methods

6.2.1 Propagation and inactivation of virus

The following work was done in containment level 3 at VIDO-InterVac, including plaque assay and inactivation described later on. MDCK cells were grown in T150 flasks to confluency. Both A/Alberta/01/2014 H5N1 and A/BC/01/2015 H7N9 viruses, provided by the National Microbiology Laboratory in Winnipeg, Manitoba, were infected at a multiplicity of infection (MOI) of 0.001, and the virus inoculum was incubated on the cells for 1 hour at 37°C with 5% CO_2. The cells were then rinsed and viral growth media, basal minimum essential medium eagle (Sigma, RNBF4696) with 0.25% BSA (Sigma, A7906-100g) and 1 µg/ml TPCK trypsin (Affymetrix, 9002-07-7), was added to the cells. Cells were then incubated for 48 hours at 37°C with 5% CO2, which is the length of time needed to see 100% cytopathic effect. At this point the supernatant was harvested and spun down briefly to remove any cell debris. β-propiolactone (Sigma-Aldrich, P5648) was added at a dilution of 1:2000 to the viral supernatant for inactivation. The viral supernatant was then incubated overnight with the β-propiolactone, rocking at 4°C. Once the inactivation procedure was complete it was stored at -80°C.

6.2.2 Plaque assay

A plaque assay was done to confirm that inactivation with β-propiolactone was successful and to determine the virus titre prior to inactivation. For inactivation confirmation MDCK cells in a 6-well plate, in duplicate, were infected with a 1 in 100 dilution of inactivated virus or mock

infected. To determine virus titre MDCK cells were plated in 6-well plates and the cells were infected with 10^{-5}, 10^{-6}, and 10^{-7} dilutions of each virus in duplicate. Plates were Incubated for one hour with the inoculum at 37°C with 5% CO_2. Agar mixed with viral growth media was then added to the cells after the inoculum was removed and let stand for ten minutes until the agar started to solidify. Plates were then placed in the incubator for 48 hours at 37°C with 5% CO_2. After incubation the agar is removed and coomassie blue is added to the cells for ten minutes. The coomassie blue is then rinsed off with reverse osmosis treated water and the plate can be left to dry on paper towel. After drying the plate can be examined for plaques.

6.2.3 Virus purification

Once the viruses were confirmed inactivated they were decontaminated out of the CL3 laboratory using proper disinfectant, microchem plus (National Chemical Laboratory Inc., 0255) with a 10-minute contact time, and brought to the CL2 laboratory for purification. Purification was done using ultra-centrifugation with a sucrose gradient. First the inactivated viral supernatant is ultra-centrifuged at 25000 rpm for 2 hours and 30 minutes at 4°C to form a pellet of un-purified virus. The supernatant of the pelleted virus is removed and 1 ml of TSE buffer (0.02 M Tris, 0.15 M NaCL, and 0.002 M EDTA-Na in ddH_2O) is added. The pellet is then left overnight at 4°C to allow for it to soften. The next day you make a sucrose gradient using 60% and 30% sucrose in TSE buffer, with the 30% sucrose layered on top of the 60% sucrose. The virus pellet is then re-suspended and added to the top of the sucrose gradient. The virus and sucrose gradient are then centrifuged at 25000 rpm for 2 hours and 30 minutes at 4°C. Purified virus can then be visualized at the sucrose/sucrose interface and is removed using a 2 ml plastic pipette and moved to a new tube. TSE buffer is added to the purified virus to wash and remove any residual sucrose from the sample and then ultra-centrifuged for 1 hour 30 minutes at 35000

rpm, 4°C. The supernatant is then removed and 0.5 ml TSE buffer is added to the pellet and it is left overnight at 4°C to soften. The next day the pellet is re-suspended in TSE buffer and additional TSE buffer is used to wash the walls of the tube, total volume around 1.5 ml. The purified virus can then be aliquoted out and stored at -80°C.

6.2.4 Ethics statement

In accordance with the Guidelines of the Canadian Council on Animal Care and with the University of Saskatchewan Committee on Animal Care and Supply all animals were treated and cared for in compliance with the 3R principles at VIDO-InterVac, University of Saskatchewan. The following experiment was approved by the University of Saskatchewan Animal Ethics Board.

6.2.5 Vaccine mouse trial

Thirty-five six-week-old naïve female BALB/c mice were used in this study. Animals were divided randomly into seven groups of 5 animals. The groups are as follows; PBS control group, inactivated H5N1 vaccine, inactivated H7N9 vaccine, inactivated H5N1 vaccine plus RNA-LZ-1, inactivated H7N9 vaccine plus RNA-LZ-1, inactivated H5N1 vaccine plus VIDO triple adjuvant, and inactivated H7N9 vaccine plus VIDO's triple adjuvant. Similar with previous trials RNA-LZ-1 was complexed with in-vivo jetPEI to reduce degradation once injected and 5 µg of RNA-LZ-1 was injected per mouse. For both of the antigens 1 µg of HA protein was used per mouse. On day 0 after 7 days of acclimation animals were pre-bled and then injected intra-muscularly with 25 µl of vaccine per leg into the semi-membranous muscle. Fourteen days after the first injection animals were bled for serum and then given a booster of the same vaccination. Ten days after the boost animals were bled and sacrificed.

6.2.6 Hemagglutinin inhibition assay

Serum from the vaccinated animals was treated with receptor destroying enzyme (RDE) (Sigma-Aldrich, C8772), diluted 1 in 20 in calcium saline pH 7.2, and incubated overnight at 37°C. The next day 1.5% sodium citrate was added to the serum and the mixture was incubated at 56°C for 30 minutes to inactivate the RDE. Next the serum is treated for 1 hour at 4°C with 50% red blood cells (RBC) from chicken to reduce nonspecific agglutinations. When the incubation period was over tubes were briefly centrifuged and cleared serum was moved to a new tube. The serum is now ready to be used for the assay.

In a 96-well plate serum samples were serially diluted 2-fold through wells A-H. Standardized antigen, 4 HA units of the designated virus, was added to every well. The serum and standardized antigen were allowed to incubate together for 1 hour at room temperature. After the incubation time 1% RBCs were added to every well and the plate was observed after 30 minutes incubation at room temperature for the formation of buttons. Formation of a button, the RBCs pooled at the bottom of the well, indicates that the serum has enough antibodies present to inhibit the hemagglutination by the virus.

In a 96-well plate serum samples were serially diluted through wells A-H. Standardized antigen, 4 HA units of the designated virus, was added to every well. The serum and standardized antigen were allowed to incubate together for 1 hour at room temperature. After the incubation time 1% RBCs were added to every well and the plate was observed after 30 minutes incubation at room temperature for the formation of buttons. Formation of a button indicates that the serum has enough antibodies present to inhibit the hemagglutination by the virus.

6.2.7 IgG antigen-specific ELISA

The day before the assay was performed a 96-well plate is coated with 2.5 μg/ml of antigen, either inactivated H5N1 or H7N9 virus, in coating buffer (0.015 M $NaCO_3$, 0.035 M $NaHCO_3$ in ddH_2O, pH 9.6) and left at 4°C overnight. The coating antigen was then removed from the plate and the plate was washed 4 times in 1xTBST (0.1 M Tris, 0.17 M NaCl, 0.05% Tween 20 in ddH_2O) before blocking buffer (1% skim milk in 1 × TBST) was added to the plate and incubated for 1 hour at room temperature. After blocking the plate was washed again 4 times and then the serum samples were added. In the first well a 1 in 40 dilution of serum was added, the serum was then serially diluted 4 times down the rows (wells A – H) in 0.5% skim milk in 1 × TBST. The serum was then incubated on the plate for 1.5 hours at room temperature. After washing the plate a 1 in 5000 dilution of phosphatase labeled reserveAP anti-mouse IgG antibody (KPL, 0751-1806) in 0.5% skim milk in 1 × TBST was added to all wells and allowed to incubate at room temperature for 1 hour. Finally, PNPP substrate diluted 100 times in PNPP buffer (1% diethanolamine, 0.5 mM $MgCl_2$ in ddH_2O) was added to develop the plates. After 20 minutes of incubation at room temperature the plates were read at 405 nm with a 490 nm reference filter.

6.2.8 Statistical analysis

Statistical analysis was done using a two way ANOVA with multiple comparison between each time point to the designated mock group in GraphPad Prism software.

6.3 Results

6.3.1 Ability of RNA-LZ-1 to produce an H5N1-specific antibody response

For this experiment, we paired RNA-LZ-1 and VIDO's triple adjuvant with two different antigens, inactivated H5N1 and H7N9 avian influenza A viruses. The H5N1 inactivated

whole virus had low immunogenicity on its own (Figure 11) so the addition of an adjuvant was essential in producing protective antibodies. The addition of either RNA-LZ-1 or the triple adjuvant significantly increased both antigen-specific IgG antibodies (Figure 11A) and neutralizing antibodies (Figure 11B) after one or two doses of the vaccines. Both the IgG titre and hemagglutinin inhibition (HAI) titre showed us similar patterns indicating strength in our results. After the prime vaccination antigen-specific antibodies were not significantly induced compared to the mock group for either RNA-LZ-1 or VIDO triple adjuvant paired groups. However, after both the prime and boost vaccination both groups adjuvanted with either RNA-LZ-1 (Figure 11B; $p=0.05$) or VIDO's triple adjuvant (Figure 11B; $p<0.0001$) had significantly increased H5N1-specific IgG titres. For HAI, RNA-LZ-1 significantly induced the titre in comparison to the mock after both prime and boost vaccinations (Figure 11B; $p<0.0001$). This result was also seen for the VIDO triple adjuvant paired H5N1 group (Figure 11B; $p<0.0001$). Classically for the HAI assay, a hallmark assay of influenza vaccine protection, a titre ≥ 40 was considered protective (Baz, Luke, Cheng, Jin, & Subbarao, 2013; Sun et al., 2017), however, recently for H5N1 specifically it has been shown that HAI titres as low as 10 or 20 are sufficient to provide protection against challenge (Mahmood et al., 2008; Pearce et al., 2012). Based on these reports we can state that RNA-LZ-1 when paired with an H5N1 antigen is capable of producing protective HAI antibody titres. RNA-LZ-1 when compared to VIDO's triple adjuvant can be said to be just as efficient at producing antigen-specific antibodies. These results indicate that RNA-LZ-1 has the potential to be an effective adjuvant when paired with vaccines against H5N1 avian influenza A virus strains.

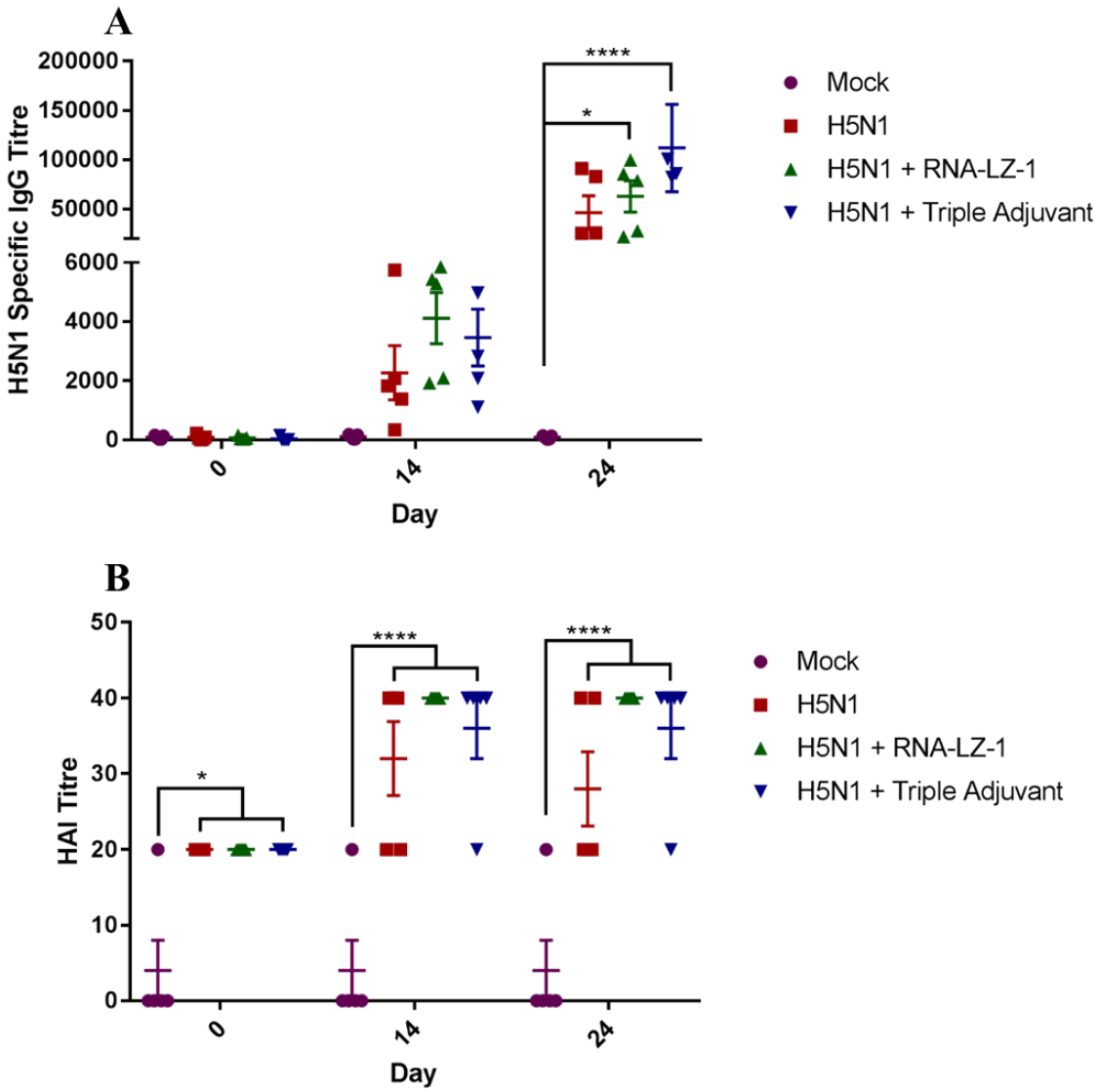

Figure 11: Vaccination with inactivated H5N1 influenza virus paired with an adjuvant led to an increased antibody response. Serum was collected from animals at three different time points, prior to vaccination and at necropsy (n=5). Plates were coated with H5N1 antigen and goat anti-mouse IgG antibody was used to detect antigen specific IgG (A). Serum was serially diluted and H5N1 virus was added to determine the titre of hemagglutinin inhibition (B). Statistical analysis was done using a two-way ANOVA (* $p=0.05$, **** $p<0.0001$).

6.3.2. Ability of RNA-LZ-1 to induce H7N9-specific antibody response

Compared to our H5N1 results (Figure 11) the vaccine combinations against H7N9 proved to have an unexpected result. Unlike the H5N1 strain H7N9 can be fairly immunogenic on its own. In the case of our trial the H7N9 inactivated whole virus alone was capable of inducing an IgG titre (Figure 12A; $p=0.05$) and protective HAI titres after the boost vaccination (Figure 12B; $p=0.001$). The addition of VIDO's triple adjuvant led to the expected results of significantly increased antigen-specific IgG titres (Figure 12A; $p<0.0001$) and producing a protective HAI titre (Figure 12B; $p<0.0001$). However, unlike what we expected the addition of RNA-LZ-1 as an adjuvant appeared to have a negative effect on the antigen-specific antibody titres. For the HAI titres (Figure 12B) even though the RNA-LZ-1 group had protective antibody levels ≥ 40 in relation to the H7N9 inactivated virus alone it was not more protective. This pattern of results can also be observed in the antigen-specific IgG titres (Figure 12A). After comparing the RNA-LZ-1 adjuvanted H7N9 group to the previous H5N1 group it leads to questions about the results seen in Figure 12. One case may be that since H7N9 alone is so immunogenic the addition of RNA-LZ-1 led to a cytokine storm, an excessive release of pro-inflammatory cytokines, decreasing the induction of antigen-specific antibodies. Another factor could be the length of time between the prime and boost vaccinations. In our case there was a 2 week spread between vaccinations, if the time between the 2 vaccinations was increased it may allow the immune response to dip back down to basal levels before peaking with the boost vaccination. Instead it is possible that the immune response in the mice was still decreasing when the booster was given, leading to a heightened response and possible cytokine storm.

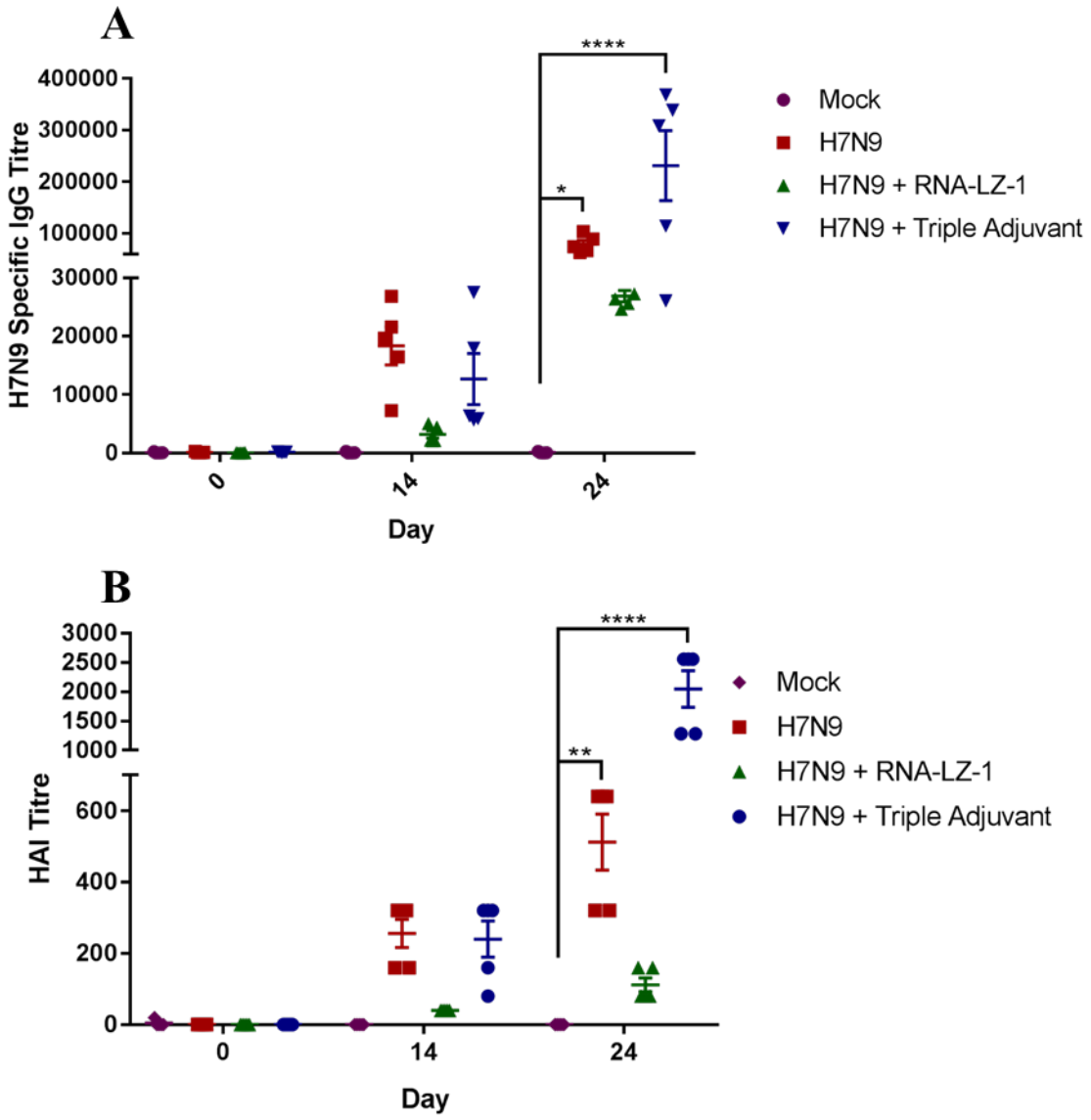

Figure 12: Vaccination with inactivated H7N9 influenza virus paired with the triple adjuvant led to an increased antibody response. Serum was collected from animals at three different time points, prior to vaccination and at necropsy (n=5). Plates were coated with H7N9 antigen and goat anti-mouse IgG antibody was used to detect antigen specific IgG (A). Serum was serially diluted and H7N9 virus was added to determine the titre of hemagglutinin inhibition (B). Statistical analysis was done using a two-way ANOVA (* p=0.05, ** p= 0.001, **** p<0.0001).

6.4 Discussion

Vaccination for H5N1 with RNA-LZ-1 as an adjuvant led to a significantly increased antigen-specific antibody production. This result proved that RNA-LZ-1 has the potential to be a potent adjuvant against RNA viruses. In comparison to VIDO's triple adjuvant RNA-LZ-1 significantly increased antibody titres to similar levels against H5N1. Over the last couple years avian H5N1 has become a pandemic threat due to its high level of mortality in humans directly infected from poultry, and due to the fact that influenza mutates so rapidly it may soon achieve sufficient transmissions in humans (Webster & Govorkova, 2006). Therefore, the fact that RNA-LZ-1 was able to significantly increase antibody responses and that the mechanism of action is known makes RNA-LZ-1 a candidate for future testing as an adjuvant. Since there was no challenge study in these results, due to regulatory factors, it is imperative to perform a challenge study to solidify RNA-LZ-1 efficacy as an adjuvant candidate.

For H7N9 vaccination it was found that VIDO's triple adjuvant was able to significantly increase antibody response compared to the un-adjuvanted vaccine. In comparison, the addition of RNA-LZ-1 was detrimental on the antibody protection induced by a prime boost vaccination regime. This half of the trial will need to be repeated in order to confirm whether our results were correct and RNA-LZ-1 is downregulating the antibody response or if there is a secondary reason why this result was observed. Whether a cytokine storm is being produced or there needs to be increased time between the prime and boost vaccinations.

Chapter 7 Discussion and conclusions

Currently there is a significant need for vaccines, which are highly immunogenic and have a strong safety profile. A major strategy for enhancing immunogenicity is the addition of an adjuvant. Recently more experimental adjuvants acting on pattern recognition receptors (PRR) have been discovered. Many viruses trigger different PRRs, which lead to not only the inhibition of the virus but also to the development of an adaptive immune response (Martinez-Gil et al., 2013). These adjuvants which act on the PRRs utilize this phenomenon triggering a similar immune response to that of natural infection via the viruses. Common PRRs targeted by adjuvants being developed are toll like receptors (TLR) and RIG-I like receptors (RLR). Adjuvants targeting TLR pathway activation include; TLR4 by AS03 (Alving et al., 2012), TLR9 by CpG (Hemmi et al., 2000), and TLR3 by polyI:C (Ishii, Koyama, Nakagawa, Coban, & Akira, 2008). The activation of RLRs by experimental adjuvants include; polyI:C activating MDA5 (Ishii et al., 2008), copy back defective interfering RNA derived from Sendai virus and RIG-I (Martinez-Gil et al., 2013), microRNA-136 and RIG-I (Zhao et al., 2015), M8 and RIG-I (Beljanski et al., 2015), 3pRNA and RIG-I (Hochheiser et al., 2016), and RNAdjuvant and RIG-I (Ziegler et al., 2017). Since the stimulation of these PRRs mimic natural infection the signals produced can directly or indirectly increase the presence of antigen-presenting cells (APCs) through cytokine and chemokine induction (Desmet & Ishii, 2012), therefore, increasing the adaptive immunity to the paired antigen. This type of adjuvant tends to produce a Th1 skewed response due to the induction of pro-inflammatory cytokines and will be beneficial to vaccines against pathogens requiring a cell-mediated immune response, such as influenza A (Beljai et al., 2015; Ziegler et al., 2017). Therefore, this study determined whether a new small RNA molecule, RNA-LZ-1, which binds to the cytosolic receptor RIG-I was capable of inducing a

broad spectrum immune response and lead to protective antibody response to a paired antigen against influenza A virus.

Previously in our laboratory it was determined that the panhandle structure derived from the 3' and 5' non-coding regions of the influenza A genome, which is highly conserved, had a strong binding affinity for RIG-I (G. Liu et al., 2015). We opted to explore whether this small RNA molecule, RNA-LZ-1, was capable of becoming a prospective adjuvant. Based on previous research of RIG-I agonists showing increased protection in mice challenged with RNA viruses (Beljanski et al., 2015; Cao et al., 2016; Hochheiser et al., 2016; Martinez-Gil et al., 2013; Ziegler et al., 2017) we expected that our RIG-I agonist would be a potent inducer of inflammatory immune response and lead to protective antibodies against a paired antigen. We first confirmed *in vitro* that RNA-LZ-1 was indeed inducing the RIG-I pathway. Human macrophages and lung epithelial cells were transfected with RNA-LZ-1 or the known RIG-I inducer, polyI:C, and supernatant and cell lysis were collected 18 hours after transfection. ELISA and qPCR were used to analyze IFN-β at the protein and mRNA level respectively. As expected RNA-LZ-1 was capable of inducing significant levels of expression higher than or equal to that of polyI:C. At the protein level we also determined that RNA-LZ-1 was capable of inducing inflammatory cytokines in transfected cells. RNA-LZ-1 was confirmed to be a potent inducer of type-I IFNs due to its ability to stimulate a more robust immune response in comparison to polyI:C. Previous results with the M8 RIG-I agonist derived from vesicular stomatitis virus, which was proven to be protective in a mouse model, showed induction *in vitro* of both IFN-β and IL-6 similar to RNA-LZ-1 (Chiang et al., 2015). Therefore, due to the similarity in *in vitro* responses between M8 and RNA-LZ-1 we could justify moving into an *in vivo* mouse model to test whether this robust immune response detected in cell culture could be replicated *in vivo*.

As suspected, *in vivo* RNA-LZ-1 was able to induce a broad spectrum immune response in injection site tissue. Since RNA-LZ-1 has never been tested in the mouse model it was important to determine the optimal dose for immune response induction. Based on previous research with a RIG-I agonist (Beljanski et al., 2015) we chose our dosage range to be 1 μg, 2.5 μg, and 5 μg. The 5 μg dose of RNA-LZ-1 was the most proficient inducer of inflammatory genes, 5 μg was the same concentration used in previous studies in BALB/c mice with a RIG-I agonist derived from vesicular stomatitis virus (Beljanski et al., 2015). An up-regulation of IFN-β, pro-inflammatory cytokines, and immune cell recruitment genes were observed, indicating that the optimal dose *in vivo* was 5 μg of RNA-LZ-1. The resulting inflammatory gene profile suggested a skewed Th1 response. The next logical step was to determine the kinetics of RNA-LZ-1 *in vivo* to profile the immune response. RNA-LZ-1 induced an immune response early on post-injection dissipating by 48 hours. The majority of genes were up-regulated at 6 hours post-injection and returned to basal levels by 24 to 48 hours post-injection. Due to this pattern many genes not up-regulated during the dosage trial were observed in the kinetics trial. The majority of genes found to be up-regulated by RNA-LZ-1 *in vivo* have been previously characterized as genes differentially expressed by RIG-I (Goulet et al., 2013). Based on the previous analysis (Goulet et al., 2013) we can conclude that RNA-LZ-1 up-regulates genes in the following functional categories; chemokines, type-I IFN, and pro-inflammatory cytokines. In future studies it would be beneficial to check genes related to the activation of the NF-κB pathway and IFN regulatory factor signalling, however, based on the downstream production of IFNs, cytokines, and chemokines we can suspect that these pathways are being activated. The genes up-regulated by RNA-LZ-1 through the RIG-I pathway indicate a skewed Th1 immune response, leading to the clearance of intracellular pathogens, however, over stimulation of pro-inflammatory

cytokines can have a negative effect on the host cells (Berger, 2000). To prevent an excessive cytokine response, or cytokine storm, the body has a mechanism to regulate this response, hence the Th2 immune response. Th2 immune response produces many cytokines and interleukins important for antibody production and eosinophil activation, however, it also produces the anti-inflammatory cytokine IL-10 which is capable of counteracting the Th1 response (Berger, 2000). At 6 hours post-injection we see a spike in IL-10 up-regulation, this may be activated in order to control the Th1 response and not cause a cytokine storm. Based on the promising gene profile collected from the kinetics trial we wanted to compare our results to the gene profile of a known adjuvant.

VIDO's triple adjuvant has been shown to increase the efficacy of a subunit vaccine against respiratory syncytial virus (Garg et al., 2014). Following the same procedure as the RNA-LZ-1 kinetics trial mice were injected intra-muscularly and tissue samples were collected at 6 and 24 hours post-injection. Similar to RNA-LZ-1 the triple adjuvant induced gene up-regulation early on with regulation being shut down by 24 hours and basal levels of expression observed. There was significant overlap of genes up-regulated between RNA-LZ-1 and the triple adjuvant. As expected RNA-LZ-1 was able to induce inflammatory genes similar to that of a proven adjuvant, supporting our hypothesis that RNA-LZ-1 will be an effective adjuvant.

Another RIG-I agonist is part of the triple adjuvant formulation, polyI:C, and made us question what effect RNA-LZ-1 might have when paired with the other components of the triple adjuvant, replacing polyI:C. For this injection RNA-LZ-1 was added at the same ratio as polyI:C to the other components and injected intra-muscularly. We expected the replacement of polyI:C with RNA-LZ-1 to induce similar levels of gene expression in comparison to the original triple adjuvant. However, that was not the case as the addition of RNA-LZ-1 had a detrimental effect

on gene up-regulation. All cytokines and chemokines directly linked to the RIG-I pathway were kept at basal levels. Initially we believed that the concentration of RNA-LZ-1 was too high, as 10 μg was added to replicate the amount of polyI:C in VIDO's triple adjuvant, as many paper utilizing RIG-I agonists worked with a maximum concentration of 5 μg per mouse (Beljanski et al., 2015; Hochheiser et al., 2016; Martinez-Gil et al., 2013). However, after searching the literature more, 3 papers were recovered, which utilized higher concentrations of RIG-I agonists without the negative response observed in our trial (Cao et al., 2016; Goulet et al., 2013; Ziegler et al., 2017). Although in all of these papers the RIG-I agonist was not complexed with other compounds, therefore, it is possible that the combination of peptide and EP3 with RNA-LZ-1 is not compatible. Based on these results only RNA-LZ-1 and VIDO's triple adjuvant were continued with for the vaccine trial.

In the host RIG-I is responsible for the detection of viruses from the following families *orthomyxoviridae, paramyxoviridae, rhabdoviridae, and flaviviridae* (Kato et al., 2006; Ranjith-Kumar et al., 2009; Sumpter et al., 2005; Yoneyama et al., 2004). The host requires a cell-mediated immune response in order to combat viruses from these families. In the case of cell-mediated immunity a Th1 immune response is needed for the production of pro-inflammatory cytokines (Berger, 2000). Based on this knowledge we chose to pair RNA-LZ-1 with avian influenza A virus strains. The highly pathogenic avian influenza A strain H5N1 and the avian influenza A strain H7N9 have in recent years spilled over the species barrier to infect humans (Cao et al., 2016; Sun et al., 2017). Though these viruses cannot sustain efficient human to human transmission, human infections are occurring from direct contact with infected poultry (Uyeki, 2009). For this study whole virus was inactivated with β-propiolactone, which was used to inactivate whole virion pandemic H1N1 vaccines ("CSL H1N1 pandemic influenza vaccine,"

2009). This trial compared the induction of antigen-specific antibodies between the inactivated whole virus with or without one of the two adjuvants, RNA-LZ-1 or VIDO's triple adjuvant. Based on our previous trials we expected RNA-LZ-1 to induce antigen-specific antibodies comparable to that of VIDOs triple adjuvant.

Animals received a prime boost vaccination regime, with two weeks between the vaccinations, and were sacrificed 10 days post-boost. Serum samples were collected prior to vaccinations and necropsy. Vaccination of inactivated H5N1 alone is known to have low antigenicity, as H5 is significantly less immunogenic compared to other hemagglutinin subtypes (Nicholson et al., 2001). The addition of an adjuvant is needed to jump this hurdle of low immunogenicity. We first did a hemagglutination inhibition assay, as it is the golden standard for determining antibody sero-protection for influenza A viruses. If the serum contains antibodies against the strain of interest it will prevent the virus from attaching to the RBCs, therefore, blocking hemagglutination. The general assumption is that an HAI titre ≥40 will provide at least a 50% reduction of influenza infection in humans (Potter & Oxford, 1979; Sun et al., 2017). The RNA-LZ-1 adjuvanted inactivated whole virus H5N1 vaccine was capable of producing an HAI titre of 40 after both the prime and boost vaccination. The vaccine adjuvanted with VIDO's triple adjuvant showed similar results. In comparison, the un-adjuvanted H5N1 vaccine was unable to produce protective antibodies against the virus. At first a HAI titre only equal to 40 seemed low but other papers have reported that HAI titres ≥10 were capable of decreasing viral replication in ferrets infected with H5N2 (Baz et al., 2013; Pearce et al., 2012). It was also shown that the H5N1 vaccine stockpiled in the U.S. only produced HAI titres of 40 in a recent study, however, the vaccine was still able to provide protection (Sun et al., 2017). These observations paired with our results indicate that for the less immunogenic H5 strains HAI titres under 40 are still able to

provide protection. The matching antigen-specific IgG antibody titre data confirmed the results showing increased antibody titres for the adjuvanted vaccines increasing after each vaccination. As expected our results showed that RNA-LZ-1 was capable of inducing a protective antibody response to the paired antigen of inactivated whole virus H5N1.

Vaccination with the inactivated H7N9 virus alone was capable of producing high levels of antigen-specific antibodies. In comparison to H5N1, H7N9 is highly immunogenic alone, however, the addition of VIDO's triple adjuvant led to significantly increased titres. After each vaccination, the titres increased for the previous two groups. In comparison, the addition of RNA-LZ-1 as an adjuvant had detrimental effects on the antibody titres, producing both HAI and antigen-specific IgG titres lower than that of H7N9 alone. This result was surprising as we expected RNA-LZ-1 to have a positive effect on antibody titres. One possible cause for this result could be that due to H7N9's immunogenicity alone the addition of RNA-LZ-1 led to a cytokine storm. This could have been aided by the shortened length of time between injections, as two weeks may have been too short for the immune response to return to basal levels before being stimulated again with the booster vaccination. However, the only way to figure out why this result occurred would be to repeat the trial. If this trail was to be repeated the length in time between prime and boost vaccination should be increased to a minimum of three weeks and a lower concentration of RNA-LZ-1 should be included to account for over stimulation of the cytokine response. Overall inactivated H7N9 whole virus with or without the addition of VIDO's triple adjuvant were able to stimulate significantly increased levels of antigen-specific antibodies.

This project was successful in proving the hypothesis correct. We showed that RNA-LZ-1 produced a robust immune response both *in vitro* and *in vivo* and was capable of inducing

significant antigen-specific antibodies against the paired antigen, inactivated H5N1 virus. Based on the data presented RNA-LZ-1 has the potential to be an adjuvant used in vaccines against viruses, which naturally trigger the RIG-I pathway. The next step for defining RNA-LZ-1 as an adjuvant would be to do a challenge trial to show whether the antibodies observed are able to provide protection against homologous challenge. At this point in time that trial was not possible for us, due to the nature of highly pathogenic avian influenza A virus research and the protocols in place surrounding animal work. Moving forwards RNA-LZ-1 will have the advantage of an adjuvant with a known mechanism of action increasing the safety profile, as unlike adjuvants such as alum, we have the knowledge behind the induction of the immune response.

Appendix

Table A1: Primers used for cytokine, chemokine, and interferon analysis by qPCR

Target gene	Direction	Sequence
IFNγ	Forward	5' TCAAGTGGCATAGATGTGGAAGAA 3'
	Reverse	5' TGGCTCTGCAGGATTTTCATG 3'
IFNα	Forward	5' CCTGTGTGATGCAACAGGTC 3'
	Reverse	5' TCACTCCTCCTTGCTCAATC 3'
IFNβ	Forward	5' ATCATGAACAACAGGTGGATCCTCC 3'
	Reverse	5' TTCAAGTGGAGAGCAGTTGAG 3'
CXCL10 (IP-10)	Forward	5' ATGACGGGCCAGTGAGAATG 3'
	Reverse	5' GAGGCTCTCTGCTGTCCATC 3'
CCL3 (MIP-1α)	Forward	5' CTTCTCTGTACCATGACACTC 3'
	Reverse	5' AGGTCTCTTTGGAGTCAGCG 3'
CCL2 (MCP-1)	Forward	5' CTTCTGGGCCTGCTGTTCA 3'
	Reverse	5' CCAGCCTACTCATTGGGATCA 3'
CXCL2 (MIP-2)	Forward	5' TGCGCCCAGACAGAAGTCATAGC 3'
	Reverse	5' GCTCTAGAGTCAGTTAGCCTTGCCTTTG 3'
CXCL1 (KC-GRO)	Forward	5' ATGAGCTGCGCTGTCAGTGC 3'
	Reverse	5' CACCAGACGGTGCCATCAGA 3'
IL-12α (p35)	Forward	5' GGTGAAGACGGCCAGAGAAA 3'
	Reverse	5' GTAGCCAGGCAACTCTCGTT 3'
IL-12β (p40)	Forward	5' GACCCTGCCCATTGAACTGGC 3'
	Reverse	5' CAACGTTGCATCCTAGGATCG 3'
TNFα	Forward	5' AGGCACTCCCCCAAAAGATG 3'
	Reverse	5' CTGCCACAAGCAGGAATGAG 3'
IL-1β	Forward	5' GTGTGGATCCCAAGCAATAC 3'
	Reverse	5' GTCCTGACCACTGTTGTTTC 3'
IL-18	Forward	5' TGGTTCCATGCTTTCTGGACTCCT 3'
	Reverse	5' TTCCTGGGCCAAGAGGAAGTGATT 3'
IL-6	Forward	5' GTGGCTAAGGACCAAGACCA 3'
	Reverse	5' TAACGCACTAGGTTTGCCGA 3'
IL-10	Forward	5' GCTGCCTGCTCTTACTGACT 3'
	Reverse	5' CTGGGAAGTGGGTGCAGTTA 3'
CCL5	Forward	5' CTCACTGCAGCCGCCCTCTG 3'
	Reverse	5' CCTTGACGTGGGCACGAGGC 3'
CCL11	Forward	5' AGAGGCTGAGATCCAAGCAG 3'
	Reverse	5' CAGATCTCTTTGCCCAACCT 3'
β-actin	Forward	5’ ACTGGGACGACATGGAG 3’

	Reverse	5’ GTAGATGGGCACAGTGTGGG 3’
GAPDH	Forward	5’ AACTTTGGCATTGTGGAAGG 3’
	Reverse	5’ ACACATTGGGGGTAGGAACA 3’
HPRT	Forward	5' GATTAGCGATGATGAACCAGGTT 3'
	Reverse	5' CCTCCCATCTCCTTCATGACA 3'

References

Alving, C. R., Peachman, K. K., Rao, M., & Reed, S. G. (2012). Adjuvants for human vaccines. *Curr Opin Immunol, 24*(3), 310-315. doi:10.1016/j.coi.2012.03.008

Awate, S., Wilson, H. L., Lai, K., Babiuk, L. A., & Mutwiri, G. (2012). Activation of adjuvant core response genes by the novel adjuvant PCEP. *Mol Immunol, 51*(3-4), 292-303. doi:10.1016/j.molimm.2012.03.026

Baz, M., Luke, C. J., Cheng, X., Jin, H., & Subbarao, K. (2013). H5N1 vaccines in humans. *Virus Res, 178*(1), 78-98. doi:10.1016/j.virusres.2013.05.006

Beljanski, V., Chiang, C., Kirchenbaum, G. A., Olagnier, D., Bloom, C. E., Wong, T., . . . Hiscott, J. (2015). Enhanced Influenza Virus-Like Particle Vaccination with a Structurally Optimized RIG-I Agonist as Adjuvant. *J Virol, 89*(20), 10612-10624. doi:10.1128/JVI.01526-15

Berger, A. (2000). Th1 and Th2 responses: what are they? *BMJ, 321*(7258), 424.

Bouvier, N. M., & Palese, P. (2008). The biology of influenza viruses. *Vaccine, 26 Suppl 4*, D49-53.

Canadian immunization guide chapter on influenza and statement on seasonal influenza vaccine for 2016-2017. (2017). 64. Retrieved from Public Health Agency of Canada website: http://www.phac-aspc.gc.ca/naci-ccni/flu-2016-grippe-eng.php

Cao, W., Liepkalns, J. S., Kamal, R. P., Reber, A. J., Kim, J. H., Hofstetter, A. R., . . . Sambhara, S. (2016). RIG-I ligand enhances the immunogenicity of recombinant H7HA protein. *Cell Immunol, 304-305*, 55-58. doi:10.1016/j.cellimm.2016.04.004

Carpenter, S., Wochal, P., Dunne, A., & O'Neill, L. A. (2011). Toll-like receptor 3 (TLR3) signaling requires TLR4 Interactor with leucine-rich REPeats (TRIL). *J Biol Chem, 286*(44), 38795-38804. doi:10.1074/jbc.M111.255893

Cha, L., Berry, C. M., Nolan, D., Castley, A., Fernandez, S., & French, M. A. (2014). Interferon-alpha, immune activation and immune dysfunction in treated HIV infection. *Clin Transl Immunology, 3*(2), e10. doi:10.1038/cti.2014.1

Chiang, C., Beljanski, V., Yin, K., Olagnier, D., Ben Yebdri, F., Steel, C., . . . Hiscott, J. (2015). Sequence-Specific Modifications Enhance the Broad-Spectrum Antiviral Response Activated by RIG-I Agonists. *J Virol, 89*(15), 8011-8025. doi:10.1128/JVI.00845-15

Cohen, J. (2013). Immunology. A once-in-a-lifetime flu shot? *Science, 341*(6151), 1171. doi:10.1126/science.341.6151.1171

Corti, D., Voss, J., Gamblin, S. J., Codoni, G., Macagno, A., Jarrossay, D., . . . Lanzavecchia, A. (2011). A neutralizing antibody selected from plasma cells that binds to group 1 and group 2 influenza A hemagglutinins. *Science, 333*(6044), 850-856. doi:10.1126/science.1205669

CSL H1N1 pandemic influenza vaccine. (2009). WHO: CSL Limited.

Desmet, C. J., & Ishii, K. J. (2012). Nucleic acid sensing at the interface between innate and adaptive immunity in vaccination. *Nat Rev Immunol, 12*(7), 479-491. doi:10.1038/nri3247

Ekiert, D. C., Bhabha, G., Elsliger, M. A., Friesen, R. H., Jongeneelen, M., Throsby, M., . . . Wilson, I. A. (2009). Antibody recognition of a highly conserved influenza virus epitope. *Science, 324*(5924), 246-251. doi:10.1126/science.1171491

Ekiert, D. C., Friesen, R. H., Bhabha, G., Kwaks, T., Jongeneelen, M., Yu, W., . . . Goudsmit, J. (2011). A highly conserved neutralizing epitope on group 2 influenza A viruses. *Science, 333*(6044), 843-850. doi:10.1126/science.1204839

Gack, M. U., Shin, Y. C., Joo, C. H., Urano, T., Liang, C., Sun, L., . . . Jung, J. U. (2007). TRIM25 RING-finger E3 ubiquitin ligase is essential for RIG-I-mediated antiviral activity. *Nature, 446*(7138), 916-920. doi:10.1038/nature05732

Galson, J. D., Truck, J., Kelly, D. F., & van der Most, R. (2016). Investigating the effect of AS03 adjuvant on the plasma cell repertoire following pH1N1 influenza vaccination. *Sci Rep, 6*, 37229. doi:10.1038/srep37229

Gamblin, S. J., & Skehel, J. J. (2010). Influenza hemagglutinin and neuraminidase membrane glycoproteins. *J Biol Chem, 285*(37), 28403-28409. doi:10.1074/jbc.R110.129809

Garg, R., Latimer, L., Simko, E., Gerdts, V., Potter, A., & van den Hurk, S. (2014). Induction of mucosal immunity and protection by intranasal immunization with a respiratory syncytial virus subunit vaccine formulation. *J Gen Virol, 95*(Pt 2), 301-306. doi:10.1099/vir.0.058461-0

Goulet, M. L., Olagnier, D., Xu, Z., Paz, S., Belgnaoui, S. M., Lafferty, E. I., . . . Hiscott, J. (2013). Systems analysis of a RIG-I agonist inducing broad spectrum inhibition of virus infectivity. *PLoS Pathog, 9*(4), e1003298. doi:10.1371/journal.ppat.1003298

Hayden, F. G., & de Jong, M. D. (2013). Human influenza: Pathogenesis, clinical features, and management In A. S. M. Robert G. Webster, Thomas J. Braciale, Robert A. Lamb (Ed.), *Textbook of Influenza* (pp. 373 - 391). The Atrium, Southern Gate, Chichester, West Sussex, UK: Jogn Wiley & Sons, Ltd.

Hemmi, H., Takeuchi, O., Kawai, T., Kaisho, T., Sato, S., Sanjo, H., . . . Akira, S. (2000). A Toll-like receptor recognizes bacterial DNA. *Nature, 408*(6813), 740-745. doi:10.1038/35047123

Hochheiser, K., Klein, M., Gottschalk, C., Hoss, F., Scheu, S., Coch, C., . . . Kurts, C. (2016). Cutting Edge: The RIG-I Ligand 3pRNA Potently Improves CTL Cross-Priming and Facilitates Antiviral Vaccination. *J Immunol, 196*(6), 2439-2443. doi:10.4049/jimmunol.1501958

Hornung, V., Ellegast, J., Kim, S., Brzozka, K., Jung, A., Kato, H., . . . Hartmann, G. (2006). 5'-Triphosphate RNA is the ligand for RIG-I. *Science, 314*(5801), 994-997. doi:10.1126/science.1132505

Impagliazzo, A., Milder, F., Kuipers, H., Wagner, M. V., Zhu, X., Hoffman, R. M., . . . Radosevic, K. (2015). A stable trimeric influenza hemagglutinin stem as a broadly protective immunogen. *Science, 349*(6254), 1301-1306. doi:10.1126/science.aac7263

Influenza Type A Viruses. (April 19, 2017). Retrieved from https://www.cdc.gov/flu/avianflu/influenza-a-virus-subtypes.htm

Ishii, K. J., Koyama, S., Nakagawa, A., Coban, C., & Akira, S. (2008). Host innate immune receptors and beyond: making sense of microbial infections. *Cell Host Microbe, 3*(6), 352-363. doi:10.1016/j.chom.2008.05.003

Jenigan, D. B., & Cox, N. J. (2013). Human influenza: One health, one world. In A. S. M. Robert G. Webster, Thomas J. Braciale, Robert A. Lamb (Ed.), *Textbook of Influenza* (pp. 3-19). The Atrium, Southern Gate, Chichester, West Sussex, UK: John Wiley & Sons, Ltd.

Kato, H., Takeuchi, O., Mikamo-Satoh, E., Hirai, R., Kawai, T., Matsushita, K., . . . Akira, S. (2008). Length-dependent recognition of double-stranded ribonucleic acids by retinoic

acid-inducible gene-I and melanoma differentiation-associated gene 5. *J Exp Med, 205*(7), 1601-1610. doi:10.1084/jem.20080091

Kato, H., Takeuchi, O., Sato, S., Yoneyama, M., Yamamoto, M., Matsui, K., . . . Akira, S. (2006). Differential roles of MDA5 and RIG-I helicases in the recognition of RNA viruses. *Nature, 441*(7089), 101-105. doi:10.1038/nature04734

Kawai, T., Takahashi, K., Sato, S., Coban, C., Kumar, H., Kato, H., . . . Akira, S. (2005). IPS-1, an adaptor triggering RIG-I- and Mda5-mediated type I interferon induction. *Nat Immunol, 6*(10), 981-988. doi:10.1038/ni1243

Kim, S. M., Kim, Y. I., Park, S. J., Kim, E. H., Kwon, H. I., Si, Y. J., . . . Choi, Y. K. (2017). Vaccine Efficacy of Inactivated, Chimeric Hemagglutinin H9/H5N2 Avian Influenza Virus and Its Suitability for the Marker Vaccine Strategy. *J Virol, 91*(6). doi:10.1128/JVI.01693-16

Klenk, H. D., Garten, W., & Matrosovich, M. (2013). Pathogenesis. In A. S. M. Robert G. Webster, Thomas J. Braciale, Robert A. Lamb (Ed.), *Textbook of Influenza* (pp. 157-173). The Atrium, Southern Gate, Chichester, West Sussex, UK: John Wiley & Sons, Ltd.

Kolakofsky, D., Kowalinski, E., & Cusack, S. (2012). A structure-based model of RIG-I activation. *RNA, 18*(12), 2118-2127. doi:10.1261/rna.035949.112

Krug, R. M., & Fodor, E. (2013). The virus genome and its replication. In A. S. M. Robert G. Webster, Thomas J. Braciale, Robert A. Lamb (Ed.), *Textbook of Influenza* (pp. 57-66). The Atrium, Southern Gate, Chichester, West Sussex, UK: John Wiley & Sons, Ltd.

Kumar, A., McElhaney, J. E., Walrond, L., Cyr, T. D., Merani, S., Kollmann, T. R., . . . Scheifele, D. W. (2017). Cellular Immune Responses of Older Adults to Four Influenza Vaccines: Results of a Randomized, Controlled Comparison. *Hum Vaccin Immunother*, 0. doi:10.1080/21645515.2017.1337615

Ladhani, L., Pardon, G., Meeuws, H., van Wesenbeeck, L., Schmidt, K., Stuyver, L., & van der Wijngaart, W. (2017). Sampling and detection of airborne influenza virus towards point-of-care applications. *PLoS One, 12*(3), e0174314. doi:10.1371/journal.pone.0174314

Lai, A. L., & Freed, J. H. (2015). The Interaction between Influenza HA Fusion Peptide and Transmembrane Domain Affects Membrane Structure. *Biophys J, 109*(12), 2523-2536. doi:10.1016/j.bpj.2015.10.044

Lassig, C., & Hopfner, K. P. (2017). Discrimination of cytosolic self and non-self RNA by RIG-I-like receptors. *J Biol Chem, 292*(22), 9000-9009. doi:10.1074/jbc.R117.788398

Lee, B. R., Jeong, S. K., Ahn, B. C., Lee, B. J., Shin, S. J., Yum, J. S., & Ha, S. J. (2016). Combination of TLR1/2 and TLR3 ligands enhances CD4(+) T cell longevity and antibody responses by modulating type I IFN production. *Sci Rep, 6*, 32526. doi:10.1038/srep32526

Lin, L., Li, Y., Pyo, H. M., Lu, X., Raman, S. N., Liu, Q., . . . Zhou, Y. (2012). Identification of RNA helicase A as a cellular factor that interacts with influenza A virus NS1 protein and its role in the virus life cycle. *J Virol, 86*(4), 1942-1954. doi:10.1128/JVI.06362-11

Liu, G., Park, H. S., Pyo, H. M., Liu, Q., & Zhou, Y. (2015). Influenza A Virus Panhandle Structure Is Directly Involved in RIG-I Activation and Interferon Induction. *J Virol, 89*(11), 6067-6079. doi:10.1128/JVI.00232-15

Liu, S., Cai, X., Wu, J., Cong, Q., Chen, X., Li, T., . . . Chen, Z. J. (2015). Phosphorylation of innate immune adaptor proteins MAVS, STING, and TRIF induces IRF3 activation. *Science, 347*(6227), aaa2630. doi:10.1126/science.aaa2630

Lyke, K. E., Burges, R., Cissoko, Y., Sangare, L., Dao, M., Diarra, I., . . . Sztein, M. B. (2004). Serum levels of the proinflammatory cytokines interleukin-1 beta (IL-1beta), IL-6, IL-8, IL-10, tumor necrosis factor alpha, and IL-12(p70) in Malian children with severe Plasmodium falciparum malaria and matched uncomplicated malaria or healthy controls. *Infect Immun, 72*(10), 5630-5637. doi:10.1128/IAI.72.10.5630-5637.2004

Mahmood, K., Bright, R. A., Mytle, N., Carter, D. M., Crevar, C. J., Achenbach, J. E., . . . Ross, T. M. (2008). H5N1 VLP vaccine induced protection in ferrets against lethal challenge with highly pathogenic H5N1 influenza viruses. *Vaccine, 26*(42), 5393-5399. doi:10.1016/j.vaccine.2008.07.084

Mahmoud, L., Al-Enezi, F., Al-Saif, M., Warsy, A., Khabar, K. S., & Hitti, E. G. (2014). Sustained stabilization of Interleukin-8 mRNA in human macrophages. *RNA Biol, 11*(2), 124-133. doi:10.4161/rna.27863

Mair, C. M., Ludwig, K., Herrmann, A., & Sieben, C. (2014). Receptor binding and pH stability - how influenza A virus hemagglutinin affects host-specific virus infection. *Biochim Biophys Acta, 1838*(4), 1153-1168. doi:10.1016/j.bbamem.2013.10.004

Martinez-Gil, L., Goff, P. H., Hai, R., Garcia-Sastre, A., Shaw, M. L., & Palese, P. (2013). A Sendai virus-derived RNA agonist of RIG-I as a virus vaccine adjuvant. *J Virol, 87*(3), 1290-1300. doi:10.1128/JVI.02338-12

McCullers, J. A. (2011). Preventing and treating secondary bacterial infections with antiviral agents. *Antivir Ther, 16*(2), 123-135. doi:10.3851/IMP1730

Meylan, E., Curran, J., Hofmann, K., Moradpour, D., Binder, M., Bartenschlager, R., & Tschopp, J. (2005). Cardif is an adaptor protein in the RIG-I antiviral pathway and is targeted by hepatitis C virus. *Nature, 437*(7062), 1167-1172. doi:10.1038/nature04193

Mosca, F., Tritto, E., Muzzi, A., Monaci, E., Bagnoli, F., Iavarone, C., . . . De Gregorio, E. (2008). Molecular and cellular signatures of human vaccine adjuvants. *Proc Natl Acad Sci U S A, 105*(30), 10501-10506. doi:10.1073/pnas.0804699105

Nichelson, K. G. (1998). Human infection. In K. G. Nicholson, R. G. Webster, & A. J. Hay (Eds.), *Textbook of Influenza* (pp. 219-264). Oxford, UK: Blackwell Science Ltd.

Nicholson, K. G., Colegate, A. E., Podda, A., Stephenson, I., Wood, J., Ypma, E., & Zambon, M. C. (2001). Safety and antigenicity of non-adjuvanted and MF59-adjuvanted influenza A/Duck/Singapore/97 (H5N3) vaccine: a randomised trial of two potential vaccines against H5N1 influenza. *Lancet, 357*(9272), 1937-1943. doi:10.1016/S0140-6736(00)05066-2

O'Hagan, D. T. (2007). MF59 is a safe and potent vaccine adjuvant that enhances protection against influenza virus infection. *Expert Rev Vaccines, 6*(5), 699-710. doi:10.1586/14760584.6.5.699

Oshiumi, H., Matsumoto, M., Hatakeyama, S., & Seya, T. (2009). Riplet/RNF135, a RING finger protein, ubiquitinates RIG-I to promote interferon-beta induction during the early phase of viral infection. *J Biol Chem, 284*(2), 807-817. doi:10.1074/jbc.M804259200

Osterholm, M. T., Kelley, N. S., Sommer, A., & Belongia, E. A. (2012). Efficacy and effectiveness of influenza vaccines: a systematic review and meta-analysis. *Lancet Infect Dis, 12*(1), 36-44. doi:10.1016/S1473-3099(11)70295-X

Palacios, G., Hornig, M., Cisterna, D., Savji, N., Bussetti, A. V., Kapoor, V., . . . Lipkin, W. I. (2009). Streptococcus pneumoniae coinfection is correlated with the severity of H1N1 pandemic influenza. *PLoS One, 4*(12), e8540. doi:10.1371/journal.pone.0008540

Patel, J. R., & Garcia-Sastre, A. (2014). Activation and regulation of pathogen sensor RIG-I. *Cytokine Growth Factor Rev, 25*(5), 513-523. doi:10.1016/j.cytogfr.2014.08.005

Pearce, M. B., Belser, J. A., Gustin, K. M., Pappas, C., Houser, K. V., Sun, X., . . . Tumpey, T. M. (2012). Seasonal trivalent inactivated influenza vaccine protects against 1918 Spanish influenza virus infection in ferrets. *J Virol, 86*(13), 7118-7125. doi:10.1128/JVI.00674-12

Peisley, A., Wu, B., Xu, H., Chen, Z. J., & Hur, S. (2014). Structural basis for ubiquitin-mediated antiviral signal activation by RIG-I. *Nature, 509*(7498), 110-114. doi:10.1038/nature13140

Potter, C. W., & Oxford, J. S. (1979). Determinants of immunity to influenza infection in man. *Br Med Bull, 35*(1), 69-75.

Ranjith-Kumar, C. T., Murali, A., Dong, W., Srisathiyanarayanan, D., Vaughan, R., Ortiz-Alacantara, J., . . . Kao, C. C. (2009). Agonist and antagonist recognition by RIG-I, a cytoplasmic innate immunity receptor. *J Biol Chem, 284*(2), 1155-1165. doi:10.1074/jbc.M806219200

Schroder, K., Hertzog, P. J., Ravasi, T., & Hume, D. A. (2004). Interferon-gamma: an overview of signals, mechanisms and functions. *J Leukoc Biol, 75*(2), 163-189. doi:10.1189/jlb.0603252

Seth, R. B., Sun, L., Ea, C. K., & Chen, Z. J. (2005). Identification and characterization of MAVS, a mitochondrial antiviral signaling protein that activates NF-kappaB and IRF 3. *Cell, 122*(5), 669-682. doi:10.1016/j.cell.2005.08.012

Sivakumar, S. M., Safhi, M. M., Kannadasan, M., & Sukumaran, N. (2011). Vaccine adjuvants - Current status and prospects on controlled release adjuvancity. *Saudi Pharm J, 19*(4), 197-206. doi:10.1016/j.jsps.2011.06.003

Skehel, J. J., & Wiley, D. C. (2000). Receptor binding and membrane fusion in virus entry: the influenza hemagglutinin. *Annu Rev Biochem, 69*, 531-569. doi:10.1146/annurev.biochem.69.1.531

Stobie, L., Gurunathan, S., Prussin, C., Sacks, D. L., Glaichenhaus, N., Wu, C. Y., & Seder, R. A. (2000). The role of antigen and IL-12 in sustaining Th1 memory cells in vivo: IL-12 is required to maintain memory/effector Th1 cells sufficient to mediate protection to an infectious parasite challenge. *Proc Natl Acad Sci U S A, 97*(15), 8427-8432. doi:10.1073/pnas.160197797

Sumpter, R., Jr., Loo, Y. M., Foy, E., Li, K., Yoneyama, M., Fujita, T., . . . Gale, M., Jr. (2005). Regulating intracellular antiviral defense and permissiveness to hepatitis C virus RNA replication through a cellular RNA helicase, RIG-I. *J Virol, 79*(5), 2689-2699. doi:10.1128/JVI.79.5.2689-2699.2005

Sun, X., Belser, J. A., Pulit-Penaloza, J. A., Creager, H. M., Guo, Z., Jefferson, S. N., . . . Tumpey, T. M. (2017). Stockpiled pre-pandemic H5N1 influenza virus vaccines with AS03 adjuvant provide cross-protection from H5N2 clade 2.3.4.4 virus challenge in ferrets. *Virology, 508*, 164-169. doi:10.1016/j.virol.2017.05.010

Thomas, K. E., Galligan, C. L., Newman, R. D., Fish, E. N., & Vogel, S. N. (2006). Contribution of interferon-beta to the murine macrophage response to the toll-like receptor 4 agonist, lipopolysaccharide. *J Biol Chem, 281*(41), 31119-31130. doi:10.1074/jbc.M604958200

Uyeki, T. M. (2009). Human infection with highly pathogenic avian influenza A (H5N1) virus: review of clinical issues. *Clin Infect Dis, 49*(2), 279-290. doi:10.1086/600035

Weber, F. (2015). The catcher in the RIG-I. *Cytokine, 76*(1), 38-41. doi:10.1016/j.cyto.2015.07.002

Webster, R. G., & Govorkova, E. A. (2006). H5N1 influenza--continuing evolution and spread. *N Engl J Med, 355*(21), 2174-2177. doi:10.1056/NEJMp068205

Xu, L. G., Wang, Y. Y., Han, K. J., Li, L. Y., Zhai, Z., & Shu, H. B. (2005). VISA is an adapter protein required for virus-triggered IFN-beta signaling. *Mol Cell, 19*(6), 727-740. doi:10.1016/j.molcel.2005.08.014

Xu, X. X., Wan, H., Nie, L., Shao, T., Xiang, L. X., & Shao, J. Z. (2017). RIG-I: a multifunctional protein beyond a pattern recognition receptor. *Protein Cell*. doi:10.1007/s13238-017-0431-5

Yoneyama, M., Kikuchi, M., Natsukawa, T., Shinobu, N., Imaizumi, T., Miyagishi, M., . . . Fujita, T. (2004). The RNA helicase RIG-I has an essential function in double-stranded RNA-induced innate antiviral responses. *Nat Immunol, 5*(7), 730-737. doi:10.1038/ni1087

Zhao, L., Zhu, J., Zhou, H., Zhao, Z., Zou, Z., Liu, X., . . . Jin, M. (2015). Identification of cellular microRNA-136 as a dual regulator of RIG-I-mediated innate immunity that antagonizes H5N1 IAV replication in A549 cells. *Sci Rep, 5*, 14991. doi:10.1038/srep14991

Ziegler, A., Soldner, C., Lienenklaus, S., Spanier, J., Trittel, S., Riese, P., . . . Kalinke, U. (2017). A New RNA-Based Adjuvant Enhances Virus-Specific Vaccine Responses by Locally Triggering TLR- and RLH-Dependent Effects. *J Immunol, 198*(4), 1595-1605. doi:10.4049/jimmunol.1601129